QUANTIFYING ATMOSPHERIC DEPOSITION OF MICROPLASTICS IN URBAN AND SUBURBAN O‘AHU

A THESIS SUBMITTED FOR PARTIAL FULFILLMENT
OF THE REQUIREMENTS FOR THE DEGREE OF

BACHELOR OF SCIENCE

IN

GLOBAL ENVIRONMENTAL SCIENCE

MAY 2025

By
IAN CHUNG

Thesis Advisor:

DR. ALISON D. NUGENT

I certify that I have read this thesis and that, in my opinion, it is satisfactory in scope and quality as a thesis for the degree of Bachelor of Science in Global Environmental Science.

THESIS ADVISOR

Alison Nugent

Dr. Alison D. Nugent
Department of Atmospheric Sciences

ACKNOWLEDGEMENTS

UROP – Provided research funding.

GES Program – Provided educational tools for success.

Andrew Garma – Assisted with lab observations.

Tianqi Zuo – Assisted with Python coding.

Carrie Tome – Provided microscope equipment.

ABSTRACT

Airborne microplastic pollution in the Hawaiian Islands can have several sources: atmospheric, oceanic, or urban. Airborne microplastic particles settle out of the atmosphere, landing in our homes, on vegetation, and all around us, where all forms of life can inhale or consume them. The primary goal of this research project is to determine the largest source of microplastic particles on Oʻahu and the impact of wind speed, wind direction, and precipitation on microplastic fallout rates. The information learned throughout the process of this research project will aid in providing the public with knowledge they can use to adjust their daily lives to limit microplastic pollution exposure and help to determine future research needs and focus future research efforts on microplastic fallout in Hawaiʻi. To determine the most significant factors for microplastic deposition, measurements of microplastic particles in two unique locations, urban and suburban, were conducted to determine the areas of Oʻahu most susceptible to atmospheric microplastic pollution. Wind speed from National Weather Service weather stations was used to contextualize the pollution measurements. While a study of this type has never been done in Hawaiʻi, prior research from other locations shows that urban centers have high fallout rates, following high wind conditions (Jahandari, 2023). Results from this project show similar results for Hawaiʻi. The data suggest that greater wind speed facilitates the dispersal of microplastics, allowing higher concentrations to accumulate in both Urban and Suburban environments. However, suburban areas have significantly lower rates of microplastic deposition regardless of weather patterns.

Keywords: Plastic, Microplastic, Atmospheric, Deposition, Wind, Precipitation

TABLE OF CONTENTS

Contents

LIST OF TABLES

LIST OF FIGURES

1.0 INTRODUCTION

1.1 PLASTIC PRODUCTION

The mass production of plastics began in the 1950s, and mankind has produced roughly 9 billion tons as of 2017 (Panko, 2017). Future projections of annual plastic production are expected to reach 34 billion metric tons, with 12 billion metric tons expected as waste (Panko, 2017). Additionally, annual production is predicted to increase exponentially (Figure 1). Plastics consist of synthetic polymers, of which there are six common types: polyethylene (PE), low-density PE (LDPE), high-density PE (HDPE), polypropylene(PP), polystyrene (PS), polyvinyl chloride (PVC), polyethylene terephthalate (PET), and polyurethane (Jadaun et al., 2022). These polymers are incorporated into everyday items such as water bottles, plastic food containers, beauty products, clothing (synthetic fibers), etc. (Ghaffar et al, 2022). Human activities also produce plastic waste from tire and brake wear, and littering (Liu et al., 2024). Once discarded, and throughout their existence, microplastics, typically between 100 nm and 5 mm in length, can degrade from their primary source and be dispersed vast distances through weather events where they interact with a diverse array of organisms, potentially contributing to the degradation of ecological function alter biogeochemical cycles (Aralappanavar et al., 2024). Though not the focus of this research, it is relevant to keep the effects of plastic pollution in mind as the factors for dispersal in Hawaiʻi are discussed.

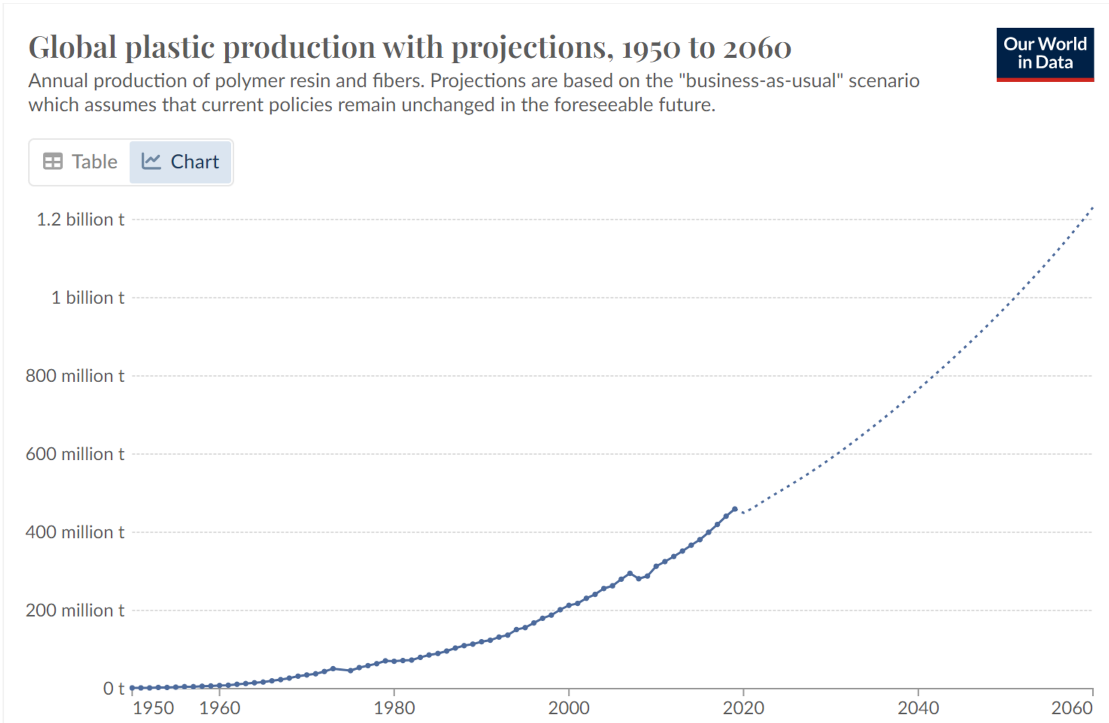

Figure 1: ***Annual Global Plastic Production Projection from 1950 - 2060 (Geyer et al., 2017; OECD, 2022)***
This graph, generated by Our World Data, a project of Global Change Data Lab, compiles data produced by Geyer et al. (2017) and the OECD to display the current global annual plastic production (darker line) and future projections (light dotted line). If current production trends remain consistent, production is expected to exceed 1.3 billion tons of plastic in 2060.

1.2 WIND-DRIVEN MICROPLASTIC DISPERSAL

Various studies discuss the potential for winds to distribute MPs across vast distances. Liu et al. (2019) and Wright et al. (2019) cite winds to be a primary and statistically significant factor in the accumulation of MPs in their samples. Furthermore, the Liu et al. (2019) and Wright et al. (2019) studies found significant correlations between microplastic counts when winds originated from urban areas. Moreover, they found that MP deposition rates increased with increasing wind speed in remote locations.

Additional findings by Allen et al. (2019) also elaborate on wind conditions that support higher rates of MP deposition, concluding that higher maximum wind speeds followed by relative periods of calm may assist in the conveyance and deposition of MP fragments. Klein and Fisher (2019) elaborate further on potential conditions that may contribute to increased rates of atmospheric MP deposition. Their study finds that storm winds or storm events, with wind speeds between 40.9 – 47.2 mph, produced the highest abundance of MPs in atmospheric fallout (Klein and Fisher, 2019). The higher wind speeds can better suspend larger-sized MP particles in the atmosphere and allow for dispersal across greater distances and into remote locations.

Once airborne, particles can circulate into and out of various environments through a cycle of suspension and resuspension driven by winds (Can-Güven, 2020, shown in Figure 2). Through this wind-facilitated process, plastics can reach great distances. Of particular interest was the quantification of the influence area of fibrous MPs and non-fibrous MPs by Wright et al. (2019). They found that fibrous MPs had a far greater dispersal area (640 – 8700 km^2) than non-fibrous MPs (186 – 875 km^2), likely due to the difference in settling velocities and deposition rates of non-fibrous and fibrous MPs. Because of their lightweight, non-fibrous MPs can make it into the most isolated places such as Alaska and Antarctic waters (Can-Güven, 2020). The range of MP dispersal implicates urban areas of Oʻahu as sources of MP pollution to Makakilo (MAK) or other remote, suburban, and rural areas, should wind conditions be favorable.

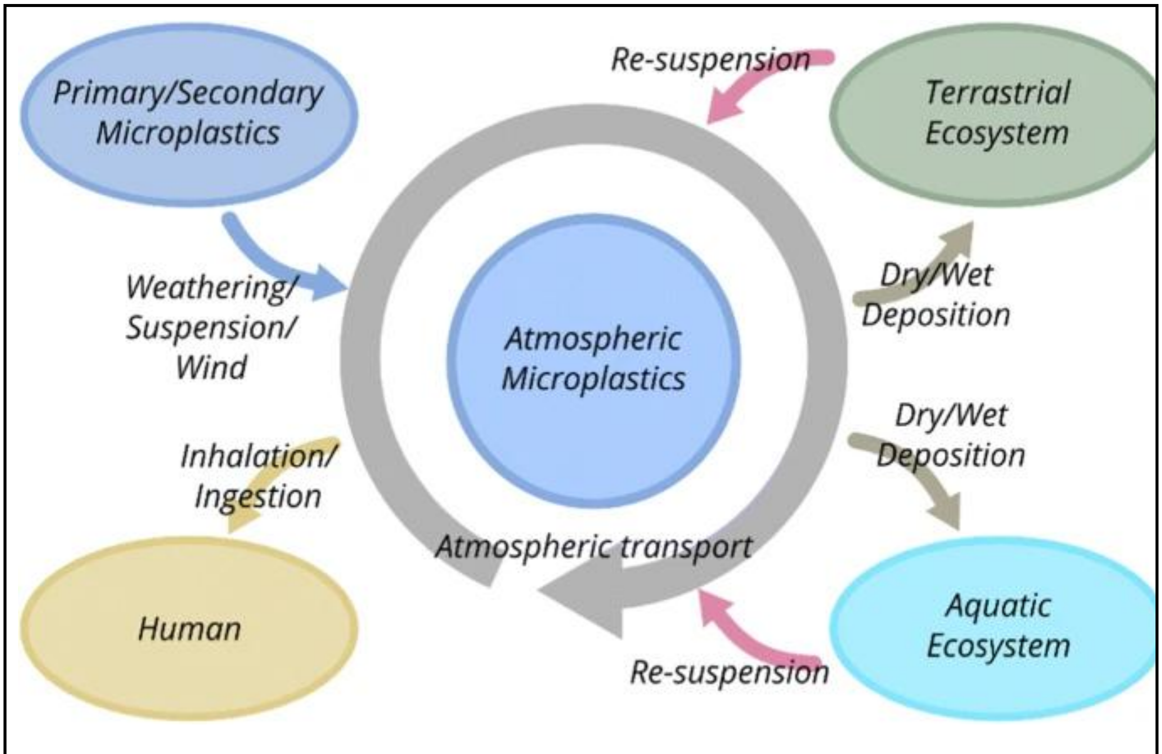

Figure 2. Possible pathways for Microplastics in the Atmosphere (Can-Güven, 2020).

MPs can be incorporated into the atmosphere and suspended by winds due to their light weight and density. Once in the atmosphere, MPs can be dispersed into aquatic and terrestrial ecosystems where they can have deleterious effects on organisms, including humans. Resuspension into the atmosphere can also occur, further distributing MPs.

1.3 PRECIPITATION STUDIES PRODUCED MIXED RESULTS

Precipitation in various forms has been correlated with higher rates of atmospheric plastic deposition in various studies. The study by Dris et al. (2016) finds a positive correlation between rainfall and MP deposition rates in urban Paris. They attribute this to being due to the abundance of synthetic clothing, degradation of macroplastics (large pieces of plastic, greater than 5 mm in size), and landfills or waste incineration in the area. Allen et al. (2019) produce similar results, but their experiment is done in the remote French Pyrenees Mountains and also incorporates snowfall into their calculations in addition to rainfall. Their study produced moderate to strong, significant positive correlations with MP counts and precipitation. In addition, they were able to distinguish that precipitation event occurrence and precipitation intensity were largely responsible for increased MP counts rather than precipitation duration. As such, the findings by Dris et al. (2016) and Allen et al. (2019) support the idea that precipitation strongly influences the deposition of MPs.

An increased MP count from precipitation could be due to sub-cloud scavenging of MPs as precipitation falls, or MPs may be incorporated into the cloud formation process as cloud or ice condensing nuclei (Aeschlimann et al., 2022). The incorporation of plastic particles in the cloud formation process, as well as the sub-cloud accumulation of plastic particles in the free troposphere by cloud precipitants, is described as a likely pathway for MPs deposition to diverse environments (Aeschlimann et al., 2022). Moreover, once aloft, wind patterns can carry clouds and MP particles vast distances, further facilitating the deposition of MPs into terrestrial or aquatic environments over greater distances (Figure 3).

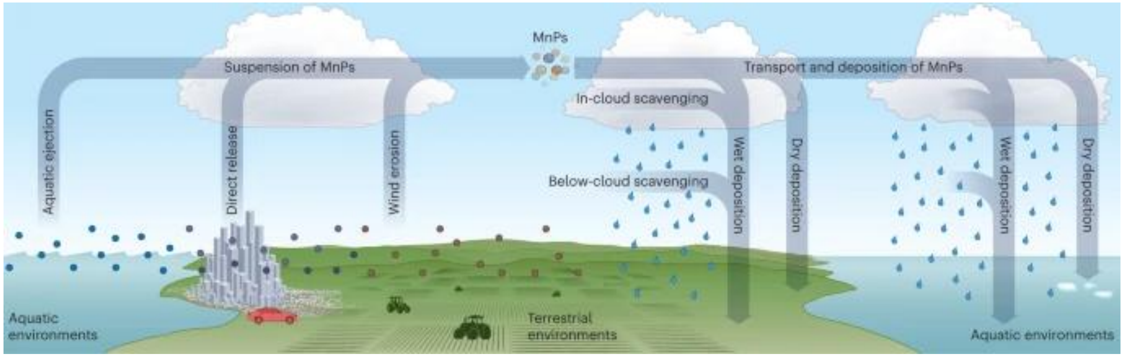

Figure 3. ***MP suspension and deposition pathways to and from terrestrial and aquatic environments (Aeschlinmann et al., 2022)***
An illustration of pathways for micro- and nanoplastic (MnPs) particles in the environment. Aeschlinmann et al. (2022) identify the ocean, urban centers, and wind erosion of plastics to be the major sources of MnP pollution. Particles from these sources can become suspended and incorporated into clouds where they precipitate, and potentially scavenge additional pollutants, eventually depositing them into other terrestrial or aquatic environments. Winds aid in the suspension and dispersal of MnPs and clouds.

1.4 OCEAN CONTRIBUTION OF MPs

Once plastics of varying sizes and compositions are deposited into the ocean, they are not likely to remain there. Allen et al. (2020) discuss the ocean's evolving role as a source of terrestrial micro- and nanoplastic pollution. Their study describes how wave and wind interactions and convective updrafts can transport plastic particles into the atmosphere. As waves crash into the ocean surface, air bubbles are created. These bubbles then make their way to the surface, burst, and subsequently expel plastic particles into the air. Furthermore, because the bubble is removed, water rushes to fill the void created by the bursting bubble, creating a secondary ejection capable of transporting larger micro-sized particles into the atmosphere. Though this process is typically associated with the transport of sea salt and organic matter, it can also atmospherically entrain micro- and nanoplastics through bubble action and jet expulsion (Allen et al., 2020). Though this process could be responsible for about 136,000 tons of plastic blowing onshore annually, recent studies have shown that the ocean acts as a sink rather than a source of MPs (Allen et al., 2020).

1.5 OCEANS PROVEN AS A MP SINK

A study by Yang et al. (2025) refutes the attribution of the ocean as a primary source of MPs to the atmosphere. Instead, their calculations suggest the ocean acts as more of a sink, accounting for roughly 15% of total deposition and 0.008% of emissions (Yang et al., 2025). To produce their results, Yang et al. incorporated laboratory simulations that analyzed the microplastic transfer between seawater and air based on sea spray aerosol formation and incorporated the findings of other studies. In tandem, Yang et al. (2025) determined that the role of the ocean as a source of MPs was overestimated by several orders of magnitude in previous studies. As such, Yang et al. (2025) adopted a model that utilized lower ocean MP emissions. Furthermore, their study discusses the size and density dependence of MP distribution, which strongly affects their settling velocity. Essentially, smaller and lighter particles can travel much further while larger and denser MPs remain closer to their source. By this rationale and including the lower ocean MP emission model, Yang et al. (2025) were able to model the net surface exchange rate of microplastic particles and identify the ocean as a sink for MPs, and coastal areas as the largest sink of MPs globally (Figure 4).

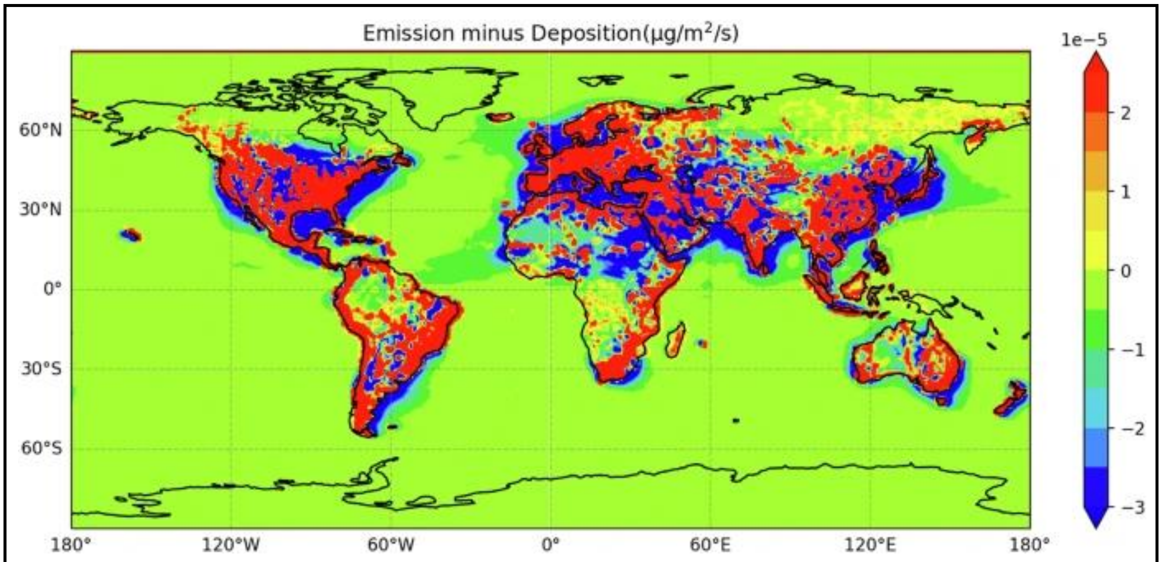

Figure 4. ***Net Surface Exchange Rate of Sub-70 µm MP particles (Yang et al., 2025)*** The net exchange rate represents the difference between the surface MP emission and deposition rates. Blue indicates a net sink and red, a source of MP emissions. Typically, coastal areas act as the most significant sink and developed land is the most significant source.

1.6 ABIOTIC DEGRADATION OF MPs

The abiotic degradation of microplastics can be achieved through mechanical fragmentation and degradation. Abiotic degradation refers to physical or chemical changes that occur through interactions with sunlight, air, temperature, and mechanical forces (Zhang et al., 2021). Mechanical fragmentation, which consists of physical interactions with plastics, occurs through abrasion and disintegration forces resulting from interactions with sediments, pebbles, waves, and tide action (Duan et al., 2021). Mechanical fragmentation can also occur in terrestrial environments through human activities such as soil cultivation and crop rotation (Duan et al., 2021). Sunlight, temperature, and air also constitute abiotic degradation. Most notably, photodegradation (degradation by sunlight) is indicated by Liu et al. (2019) to be the “most important process that initiates plastic degradation.” Overall, abiotic degradation is a significant process contributing to the formation of micro- and nanoplastic particles, which are converted to sizes that can more readily interact with and be broken down further by living organisms.

1.7 BIOTIC DEGRADATION OF MPs

Biotic degradation, the breakdown of plastics by living organisms, is another mechanism of micro- and nanoplastic particle formation (Zhang et al., 2021). Biotic degradation involves biting, chewing, or digesting plastics, reducing their size. This type of plastic degradation can also be done through biochemical processes by microorganisms, which include bacteria, fungi, and insects (Zhang et al., 2021). Microorganisms and fungi tend to break down synthetic polymers in plastics through extracellular enzymes. Because they resemble lignin, an organic polymer found in woody plants, enzymes can break down polymer chains and reduce the size of plastics through oxidation by O_2 (Zhang et al., 2021). Water can also be used to facilitate the enzymatic degradation of plastic polymers. However, both play a role in reducing the size of plastic particles, which can be small enough that microorganisms can metabolize and eventually mineralize plastics to produce various byproducts. Figure 5 illustrates the general process of biotic and abiotic degradation of plastics. Ultimately, biotic and abiotic factors contribute to the development of plastic particles of various sizes.

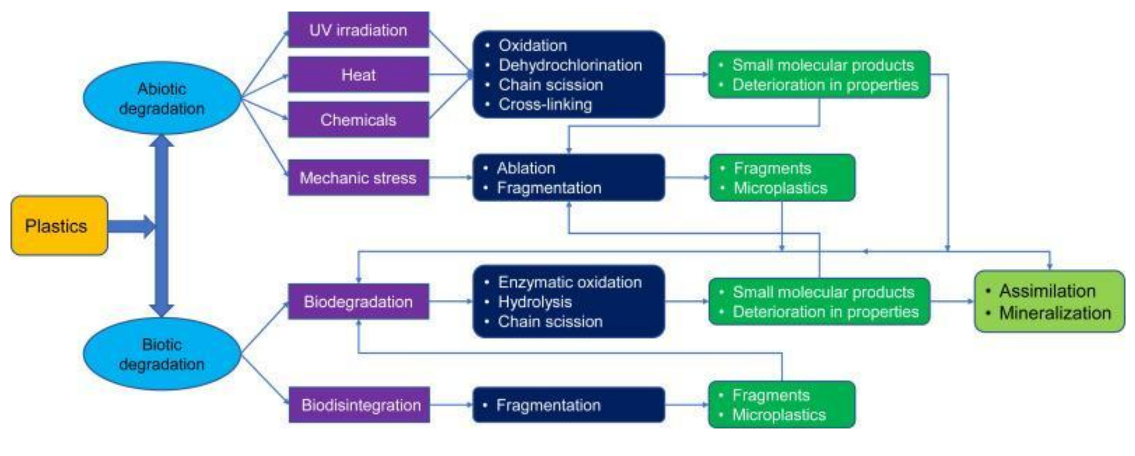

Figure 5. ***Processes of biotic and abiotic degradation of MPs (Zhang et al., 2021)*** Abiotic and biotic degradation are the primary mechanisms for breakdown of plastics into smaller particles, such as micro- and nanoplastics. Micro- and nanoparticles are between 100 nm - 5 mm and 1 nm - 100 nm, respectively, and can be easily dispersed into distant environments. Abiotic breakdown of plastics particles from their primary source is carried out by UV irradiation, heat, chemicals, and mechanical stress, while biotic degradation is facilitated by biodegradation and biodisintegration by organisms. Both processes produce microplastics, which can be assimilated by organisms of all sizes or mineralized by aquatic and terrestrial microbes (Zhang et al., 2021).

1.7 TERRESTRIAL EFFECTS OF MICROPLASTIC POLLUTION

The mineralization of plastics, a byproduct of microorganism metabolism, produces several significant compounds regarding climate change and nutrient cycles. Under aerobic conditions, the mineralization of plastics can form CO_2 and H_2O (Zhang et al., 2021). Alternatively, CH_4, CO_2, organic acids, H_2O, N_2, and N_2O form under anaerobic conditions (Aralappanavar et al., 2024). Furthermore, the introduction of plastics into the environment has been shown to alter the relative abundance of soil and aquatic microbes, potentially altering nutrient contents in some media and producing greenhouse gases (GHG) in lab experiments (Duan et al., 2021). Though these cases are produced under idealized experimental conditions, several of these gases have implications for climate change, and alterations to microbial communities could have larger implications on ecological function and nutrient content. As such, the interaction between plastics and biogeochemical cycles must be examined to determine the range of effects that plastic pollution and mineralization will have on greenhouse gas (GHG) emissions and critical ecosystem services as plastic waste of various sizes becomes ubiquitous in environments around the world.

1.8 RESEARCH INTENT

Due to Hawaiʻi's unique location within the Pacific Ocean, far from other land masses, it is vital to understand the impact of MP pollution in the diverse ecosystems of Hawaiʻi's island chain. We need to understand how MPs will impact these ecosystems and, by extension, the human population that relies on them. Moreover, Hawaiʻi's natural resources are finite and require diligent stewardship to ensure their longevity despite the growing pressures of urbanization and development. It is unfortunate that up until this point, MP experiments have not previously been conducted in Hawaiʻi or island nations. As such, this research attempts to create a foundation upon which future research can build. This endeavor sets forth, first, by quantifying atmospheric MP deposition in urban and suburban environments to determine the validity of Jahandari's (2023) experiments in the context of urban Honolulu.

2.0 METHODS

2.1 METHODS OVERVIEW

Quantifying atmospheric microplastics involves the use of several passive atmospheric deposition samplers. These samplers, used in studies by Dris et al. (2015,

2016) and described by Chen et al. (2020), are simple devices capable of collecting microplastic fallout from the atmosphere. The gathered samples are first removed from the container using distilled water and GF/A Wattman filters to separate MPs. Next, the filters with the collected MPs are processed using hydrogen peroxide (H_2O_2) and distilled water. The addition of hydrogen peroxide aids in biofouling prevention. Finally, once these steps have been completed, the total microplastics collected per sample are counted using a stereomicroscope and reported in units of MP particles m^{-2} d^{-1} (Chen et al. 2020).

2.2 SITE SELECTION

Sampling sites were selected for their difference in population densities reported as people mi^{-2}; 1,136 in MAK and 5,546 in Lower Makiki (LM) (U.S. Census Bureau, 2023). This difference allows for a proper comparison between urban and suburban areas of Oʻahu. There is also a significant elevation difference between the two sites: 314 m in MAK, and 27 m in LM. Furthermore, these sites can experience weather patterns that are unique to their location, enhancing the scope of this study, and are 25.6 km away from one another. Figure 6 displays the location of the sampling sites as well as the population density of the area.

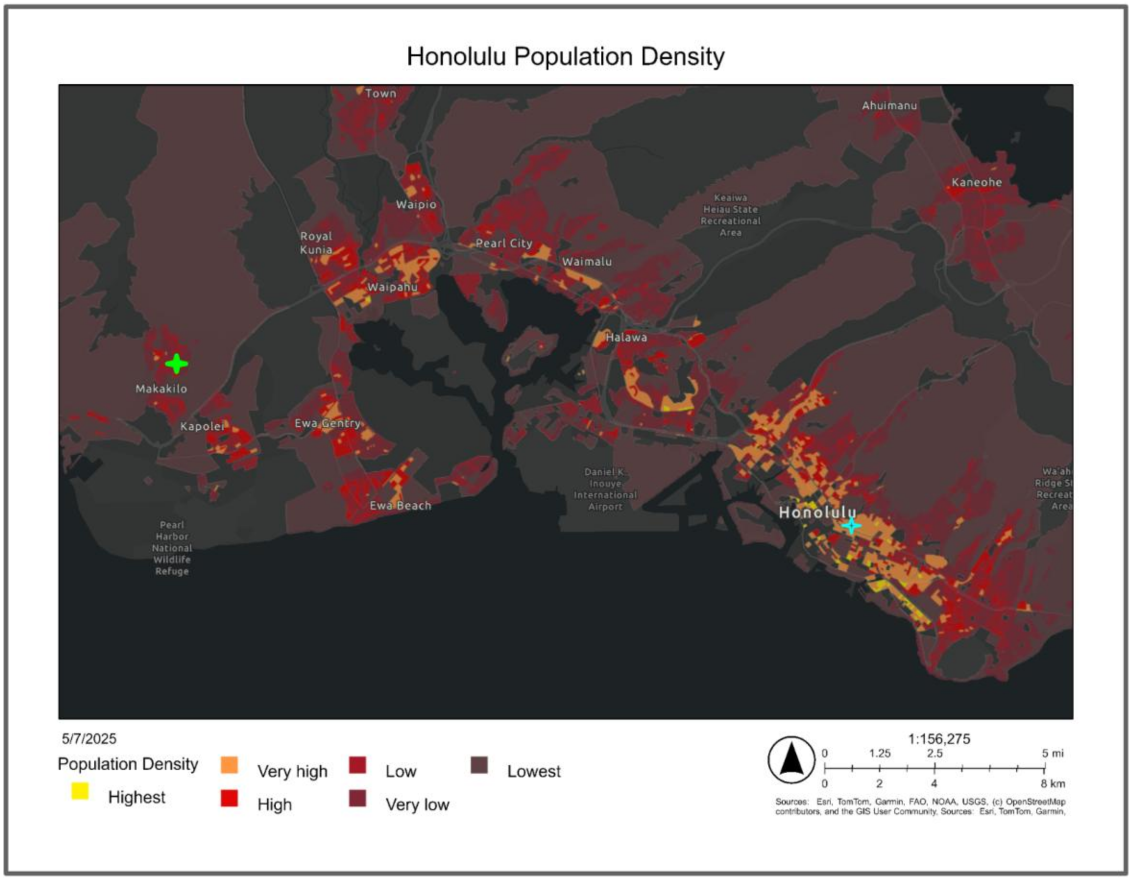

Figure 6. Sample Locations on O'ahu
The map displays the population density in people km^{-2} in the county of Honolulu. The site shown in blue corresponds with the sampling location in Lower Makiki, and the site shown in green corresponds with the Makakilo sampling location. From highest to lowest, population densities are as follows; highest: >30,000 people km^{-2} , very high: >7,000 people km^{-2}, High: >5,200 people km^{-2}, Low: >3,330 people km^{-2}, and low: >1,500 people km^{-2}.

2.3 PASSIVE SAMPLERS

A total of four passive atmospheric deposition samplers were assembled, two for each sampling location (Figure 7). Whenever possible, glass is used to eliminate sample contamination from other sources of microplastics. Once assembled, the samplers were set in LM and MAK and collected periodically from September 2024 to December 2024, a total of 9 samples at each location (18 total samples). Sample periods and collection times varied but were normalized by the number of days in subsequent calculations of selected weather variables and MP sample counts. After each week, the samplers were swapped with another set of samplers, sanitized by rinsing with distilled water, and covered to limit potential contamination. Samplers that were removed from the field location are rinsed with distilled water to gather MPs adhered to the inner surface of the sampler, then filtered through a prepped Whatman GF/A microfiber filter.

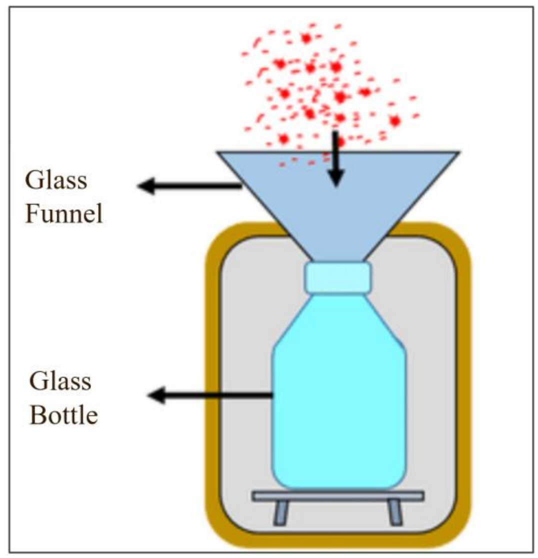

Figure 7. ***Diagram and Constructed Passive MP Deposition Sampler (Chen et al., 2020)***
Passive samplers provide time and place-specific deposition of MPs to be quantified and compared to weather variables. All components of the sampler should be glass or metal to avoid excess plastic contamination. These simple devices include a funnel and jar to collect settling MPs and precipitation. The surface area of the glass or metal funnel must be known to calculate MP deposition in particles m^{-2} d^{-1}.

2.4 FILTER PREP

Whatman GF/A 90 mm microfiber filters were used to filter out MPs from the samplers. Each filter has a 0.5 cm x 0.5 cm grid carefully drawn on the filter to aid in navigation during counting with the stereomicroscope and to easily exclude observed plastics that measure beyond micro-scale sizes (anything larger than 0.5 cm is not counted). Once the grid is applied, the filters are heated at 450°F for 15 minutes to remove any contaminants and plastics that may have accumulated during preparation. Filters are immediately placed into glass petri dishes that have also been sanitized in the same manner as the glass samplers discussed previously (Figure 8).

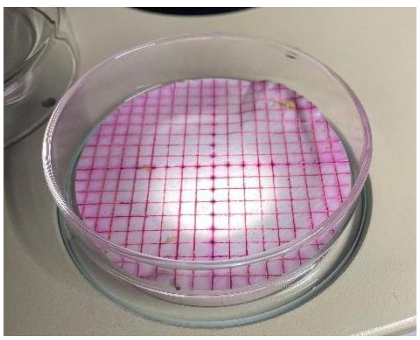

Figure 8. Prepped GF/A Whatman Glass Microfiber Filter Inside Glass Petri Dish
Filter grid lines were meticulously hand-drawn at 0.5 cm x 0.5 cm. These dimensions aided visual inspections, facilitating the easy exclusion of plastic particles that were too large to be categorized as MPs.

2.5 MICROSCOPE OBSERVATION METHODS

The model SZ3060 Olympus stereo microscope allows for counting micro-sized plastic particles less than 5 mm. However, this type of microscope and observation method limits the ability to observe nanoscale and smaller microscale plastic particles. The surface area of the funnel and exposure time are used to quantify atmospheric fallout in MP particles m^{-2} d^{-1} and are discussed in a later section (O'Brien et al., 2023). NWS wind speed measurements were concurrently recorded during the sampling periods to quantify the relationship between wind variables, precipitation, and the collected MP count. Additionally, MP counts were done independently by two counters, referred to as "Observer 1" and "Observer 2", to improve the accuracy and reliability of this study.

2.6 MICROPLASTIC IDENTIFICATION RESOURCES

To identify MPs, the Shaw Institute's Guide to Microplastic Identification was the primary reference (2019). Additional references include studies by Khuyen et al.(2022) and Gambino et al. (2022). These references organize MPs into categories illustrated in Figure 9.

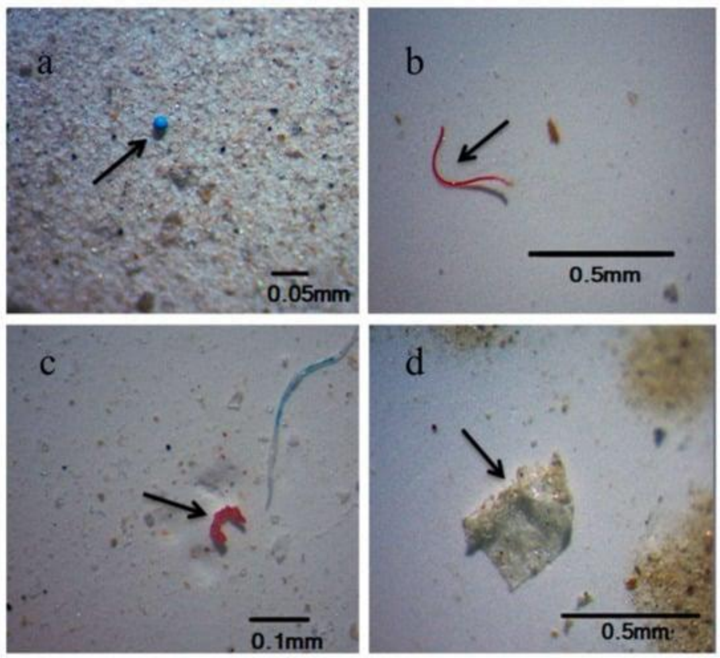

Figure 9. Common MP Filament Types: (a) pellets, (b) fibers, (c) fragments, (d) films (Gambino et al. 2022)
MPs displayed here are the primary types identified in samples. Size, color, opacity, and weathering varied.

2.7 WEATHER DATA SOURCE

Weather data used in this study was obtained from the National Centers for Environmental Information (NCEI) website. The fastest 2-minute wind speed (WSF2) and the direction of the fastest 2-minute wind (WDF2) were used as the weather variables for the MAK and LM sites. Kalaeloa Airport and Daniel K. Inouye International Airport (HNL) were used to approximate weather conditions for the MAK and LM sites, respectively. The daily values from the NCEI database for the station at Kalaeloa and HNL were then compiled into an average d^{-1} value for each site during each respective sampling period. The sample period averages for each site are displayed in Tables 1 and 2. Precipitation data were approximated from the Hawai'i Climate Data Portal website (HCDP). Daily values from HCDP were summed over the date range for each sampling period.

2.8 DATA ANALYSIS AND PLOT GENERATION

Python was utilized to conduct statistical analysis and to generate visual aids. Relevant packages include Pandas, Numpy, and Matplotlib.pyplot, Windrose, and Scipy.stats. Plots will use wind speed, direction, and precipitation as independent variables, and MP particle count as particles m^{-2} d^{-1} as the dependent variable to show any relationship between these variables. The visual aids and values generated by Python and the listed packages will be used to determine the underlying weather conditions responsible for changes in the rates of atmospheric microplastic deposition in both settings. Variables for the generated graphs include MP sample counts in particles m^{-2} d^{-1}, wind speed (WSF2), wind direction (WDF2), and precipitation. Windrose graphs are also generated to display the daily direction, speed, and frequency of the fastest 2-minute winds for each sampling period and to provide additional context of the sample periods.

2.9 DEPOSITION RATE CALCULATIONS

The surface area of the glass funnel was approximated using the formula for the surface area of a cone ($A = \pi r2 + \pi rl$). With this value, MP deposition rates from each sample period are reported as particles m^{-2} d^{-1} by dividing the average MP count by the surface area and the number of days in each sampling period. Results are recorded in Table 1. Though more sophisticated methods of quantifying deposition rates exist, this method is used so that comparisons with prior studies can be made.

Eq.1 $d = p / (sa*d)$

Here, d = deposition rate (particles m^{-2} d^{-1}), p = MP particles counted, sa = surface area (m^2), and d = number of days in the sample period.

3.0 RESULTS

3.1 HIGHER MP DEPOSITION IN LOWER MAKIKI

The results of the sampling efforts are shown in Table 1. Microplastic Counts (MPC) from September through December 2024 for both LM and MAK are shown. LM consistently has more MP counts compared to MAK. The only time this pattern is interrupted is during Samples 7 and 8.

Table 1. ***Raw Microplastic Counts at Lower Makiki and Makakilo***
Table includes (from L to R) Observer ID Numbers (observers 1 or 2), Sample ID number, Date Range per Sample (MM/DD/YYYY), Number of Days per Sample Period, Raw Counts per Sample at Lower Makiki, and Raw Counts per Sample at Makakilo.

Counter ID	Sample ID	Date Range	Days	Raw MP Counts (Lower Makiki)	Raw MP Counts (Makakilo)
1	1	09/04/2024 - 09/11/2024	7	215	91
1	2	09/11/2024 - 09/21/2024	9	187	85
1	3	09/21/2024 - 09/29/2024	9	134	68
1	4	09/29/2024 - 10/06/2024	7	114	59
1	5	10/6/2024 - 10/14/2024	8	119	79
1	6	10/14/2024 - 10/28/2024	14	127	76
1	7	10/28/2024 - 11/11/2024	14	76	82
1	8	11/11/2024 - 11/20/2024	9	61	98
~~1~~	~~9~~	~~12/24/2024 - 12/31/2024~~	~~7~~	~~159~~	~~104~~
2	1	09/04/2024 - 09/11/2024	7	190	120
2	2	09/11/2024 - 09/21/2024	9	172	118
2	3	09/21/2024 - 09/29/2024	9	110	84
2	4	09/29/2024 - 10/06/2024	7	95	146

2	5	10/6/2024 - 10/14/2024	8	127	103
2	6	10/14/2024 - 10/28/2024	14	101	72
2	7	10/28/2024 - 11/11/2024	14	81	84
2	8	11/11/2024 - 11/20/2024	9	98	113
~~2~~	~~9~~	~~12/24/2024 - 12/31/2024~~	~~7~~	~~188~~	~~121~~

**Sample 9 was excluded from data analysis because of contamination.*

Table 2 lists the average MP count between observers 1 and 2 and the corresponding deposition rate for each site. Deposition ranges from 69.1 – 356.7 MP particles m^{-2} d^{-1} were found for LM and 65.1 – 185.8 MP particles m^{-2} d^{-1} for MAK, with an average of 191.95 and 136.75 particles m^{-2} d^{-1}, respectively. The values from Table 2 also display a disruption from LM's typically higher deposition rate in Samples 7 and 8. The deposition rates from Table 2 will be used as the main dataset for all subsequent visual aids.

Table 2. ***Averaged Microplastic Counts and Deposition Rates (particles m^{-2} d^{-1}) at Lower Makiki and Makakilo.*** Table includes (from L to R) Date Range per Sample (MM/DD/YYYY), Number of Days per Sample Period, Raw Counts per Sample at Lower Makiki, and Raw Counts per Sample at Makakilo.				
Sample ID	**Averaged MP Count (Lower Makiki)**	**Deposition Rate in Lower Makiki (particles m^{-2} d^{-1})**	**Averaged MP Count (Makakilo)**	**Deposition Rate in Makakilo (particles m^{-2} d^{-1})**
1	202.5	356.7	105.5	185.8
2	179.5	245.9	101.5	139.1
3	122	167.1	76	104.1
4	104.5	184.1	102.5	180.6
5	123	189.6	91	140.3
6	114	100.4	74	65.2
7	78.5	69.1	83	73.1
8	79.5	108.9	105.5	144.5

3.2 WIND, PRECIPITATION, AND RELATIONSHIP TO MP COUNTS IN LOWER MAKIKI

Recorded values for the selected environmental variables at LM are shown in Table 3 below, and include the fastest two-minute wind speed, fastest two-minute wind direction, and rainfall per day over each sample period. Fastest wind speeds varied from 11.59 mph to 25.25 mph while the wind direction was between 59.36° to 87.99° at HNL, relatively consistent with typical trade winds. Rainfall varied from 0.45 mm to 77.23 mm at HNL.

Table *3. Honolulu Int Airport Weather Statistics*
Table includes (from L to R) sample ID, sample period (MM/DD/YYYY), Fastest 2-Minute Wind (mph), Direction of the Fastest 2-Minute Wind (Deg), and Precipitation (mm d^{-1}) and MP deposition rates (particles m^{-2} d^{-1}). Values obtained from this station are used to approximate weather conditions in the Lower Makiki Sampling site.

Sample ID	Sample period	WSF2 average (mph)	WDF2 Average (deg)	Precipitation (mm d^{-1})	Deposition Rate in Lower Makiki (particles m^{-2} d^{-1})
1	09/04/2024 - 09/11/2024	11.59	87.99°	0.0642	356.7
2	09/11/2024 - 09/21/2024	20.72	76.63°	1.16	245.9
3	09/20/2024 - 09/29/2024	22.10	69.33°	1.42	167.1
4	09/29/2024 - 10/06/2024	18.70	70.97°	2.04	184.1
5	10/06/2024 - 10/14/2024	18.92	59.36°	1.49	189.6
6	10/14/2024 - 10/28/2024	16.93	83.69°	2.56	100.4
7	10/28/2024 - 11/11/2024	21.32	66.60°	5.52	69.1
8	11/11/2024 - 11/20/2024	25.25	65.49°	2.32	108.9

In general, higher wind speeds occurred alongside lower MP counts in LM. The highest MP count (356 particles m^{-2} d^{-1}) occurred during Sample 1. This coincided with the lowest wind speed (11.59 mph) and lowest precipitation value (0.0642 mm d^{-1}), while the lowest counts, during Sample 7 were observed during the period with the largest amount of precipitation (5.52 mm d^{-1}) and relatively high wind speeds (>20 mph). These findings are visualized in Figures 10 and 11.

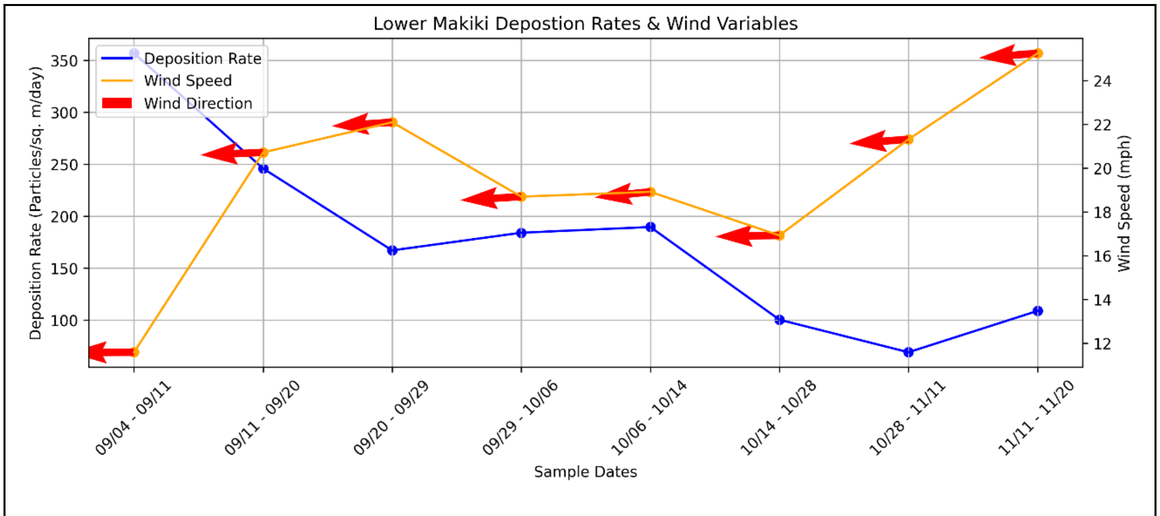

Figure 10. ***Lower Makiki Deposition Rates & Wind Variables***
This graph illustrates Lower Makiki's deposition rates in particles m^{-2} d^{-1} during each sample period in comparison to the corresponding wind speed in miles per hour and direction. The vector arrows, shown in red, illustrate the corresponding average wind direction in degrees during each sample period. As is standard, the wind direction is shown pointing in the direction the wind is headed.

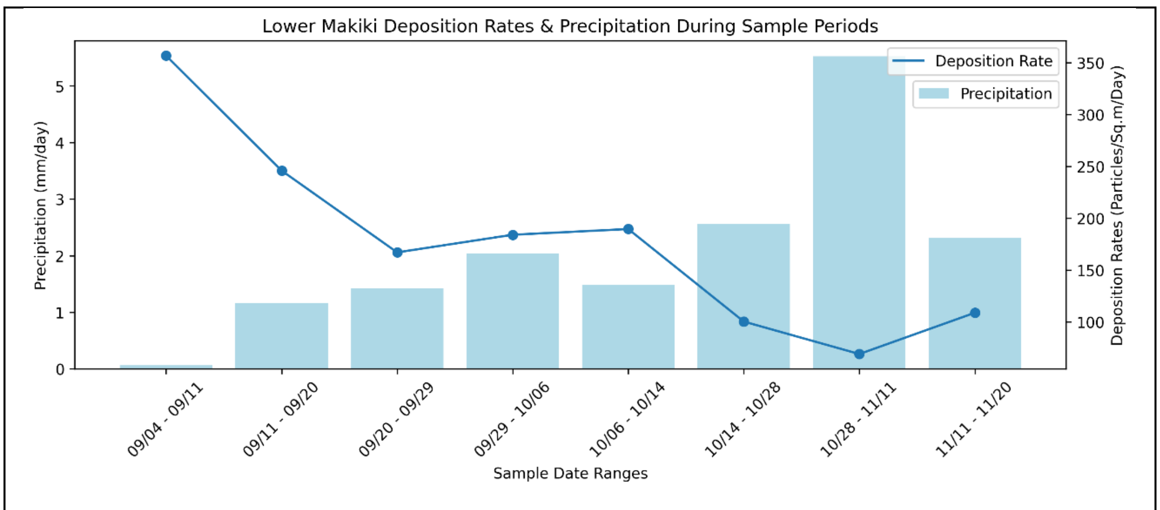

Figure 11. ***Lower Makiki Deposition Rates and Precipitation per Sample Period***
This graph illustrates the MP deposition rates (particles m^{-2} d^{-1}) in Lower Makiki alongside precipitation (mm d^{-1}).

3.2.1 ADDITIONAL LOWER MAKIKI OBSERVATIONS

Referring to Figures 10 and 11, between Samples 1 and 2, there was a decrease of 110 in the MP deposition rate per unit area and a 9.13 mph increase in wind speed.

During this period, there was also about a 1.10 mm d^{-1} increase in precipitation from the prior sample period. Another decrease in the MP deposition rate per unit area of 78.78 occurred between Samples 2 and 3. During this time, yet another increase in precipitation of about 0.26 mm d^{-1}, 1.42 mm d^{-1} total. Wind speeds also increased from 20.72 to 22.10 mph. MP deposition rates per unit area were observed to be lowest during Samples 6, 7, and 8 (100.41, 69.14, and 108.92 MP m^{-2} d^{-1}, respectively). Concurrently, these sample periods also experienced the most precipitation: 2.56, 5.52, and 2.32 mm d^{-1} respectively. Samples 6, 7, and 8 also constitute some of the highest wind speeds (16.93, 21.32, and 25.25 mph, respectively). MP deposition rates increased from Sample 7 to Sample 8. Curiously, this was during the fastest wind speed (25.25 mph) and relatively high precipitation (2.32 mm d^{-1}). In previous samples, increasing wind speeds occurred alongside decreasing MP counts.

3.3 WIND, PRECIPITATION, AND RELATIONSHIP TO MP COUNTS IN MAKAKILO

Recorded values for the selected environmental variables at MAK are shown in Table 4 below, and, like Table 3, include the fastest two-minute wind speed, fastest two-minute wind direction, and rainfall per day over each sample period. Fastest wind speeds varied from 10.48 mph to 16.49 mph while the wind direction was between 73.52° to 132.16°, showing deviations from the direction of typical trade winds. Rainfall ranged from 0.133 mm d^{-1} to 3.19 mm d^{-1}. Figures 12 and 13 display this information.

Table 4. ***Kalaeloa Weather Statistics***
Table includes (from L to R) sample period (MM/DD/YYYY), Fastest 2-Minute Wind (mph), Direction of the Fastest 2-Minute Wind (Deg), Precipitation (mm d^{-1}), and MP deposition rates (particles m^{-2} d^{-1})

Sample ID	Sample period	WSF2 Average (mph)	WDF2 Average (Deg)	Precipitation (mm d^{-1})	Deposition Rate in Makakilo (particles m^{-2} d^{-1})
1	09/4/2024 - 09/11/2024	13.20	132.16°	0.144	185.8
2	09/11/2024 - 09/21/2024	10.48	82.46°	0.133	139.1
3	09/20/2024 - 09/29/2024	12.13	79.24°	0.209	104.1
4	09/29/2024 - 10/06/2024	15.76	124.27°	0.525	180.6
5	10/6/2024 - 10/14/2024	13.01	107.61°	0.700	140.3
6	10/14/2024 - 10/28/2024	10.66	113.69°	0.943	65.2
7	10/28/2024 - 11/11/2024	11.73	78.24°	3.19	73.1
8	11/11/2024 - 11/20/2024	16.49	73.52°	0.785	144.5

The data trends for MAK's deposition rates in comparison to the selected weather variables (wind speed, direction, and precipitation) are displayed in Figures 12 and 13. Deposition rates increase with increasing wind speed. The highest recorded deposition rates (185.8 particles m^{-2} d^{-1}) occurred during Sample 1 with wind speeds at 13.1 mph and relatively low precipitation (0.144 mm d^{-1}). The lowest deposition rates were recorded in Sample 6 (65.2 particles m^{-2} d^{-1}). During this period, wind speeds were the second lowest speed recorded during the duration of this experiment. Precipitation was also elevated during this period (0.943 mm d^{-1}). Though this is the 2nd highest recorded precipitation value, it is lower in comparison to precipitation rates recorded in LM.

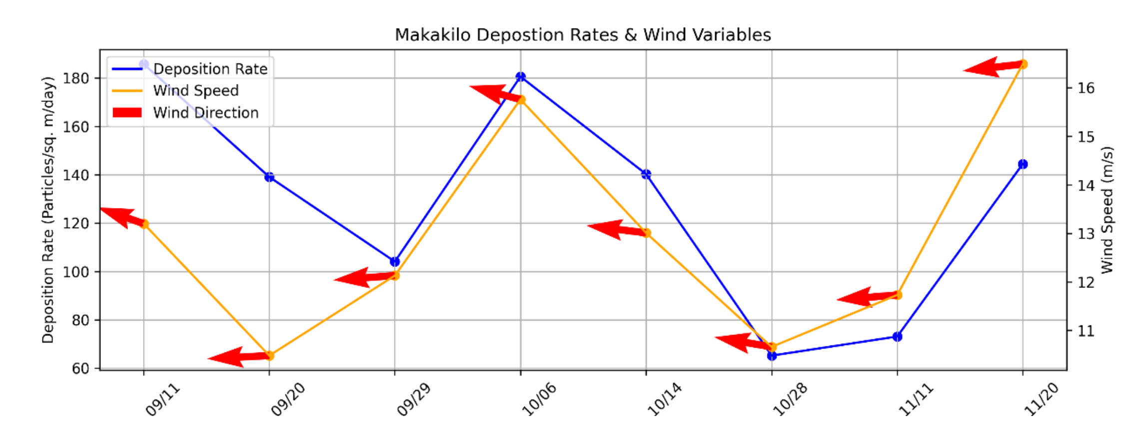

Figure 12. ***Makakilo Deposition Rates vs Wind Variables.***
This graph illustrates Makakilo's deposition rates in particles m^{-2} d^{-1} during each sample period in comparison to the corresponding wind speed in miles per hour and direction. The vector arrows, shown in red, illustrate the corresponding average wind direction in degrees during each sample period. The wind direction points in the direction the wind is headed.

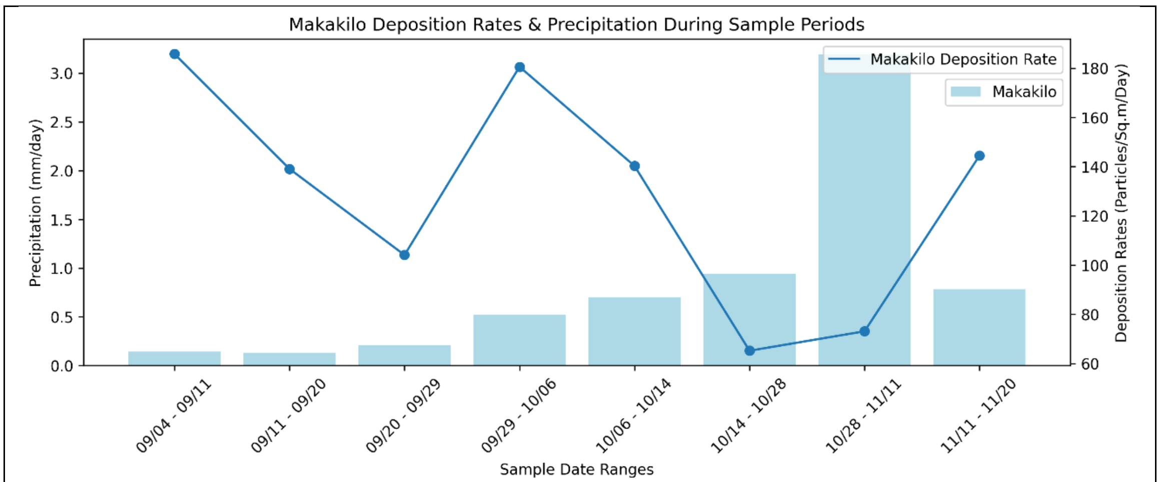

Figure 13. ***Makakilo Deposition Rates and Precipitation per Sample Period***
This graph illustrates the MP deposition rates (particles m^{-2} d^{-1}) in Lower Makiki alongside precipitation (mm d^{-1}).

3.3.1 ADDITIONAL MAKAKILO OBSERVATIONS

Referencing Figures 12 and 13, Sample 4 recorded the second largest MP count (180 particles m^{-2} d^{-1}), the 2nd highest wind speed, with relatively moderate precipitation (0.525 mm d^{-1}). During Sample 8, the precipitation rates dropped significantly (3.19 to 0.785 mm d^{-1}), and wind speed increased to the highest recorded speed (16.49 mph). Interestingly, the increased wind speed and lower precipitation coincided with another large MP deposition rate (144.5 particles m^{-2} d^{-1}), opposite to trends discussed in LM. Wind direction (>100 deg) may also have some influence on the deposition rate during Samples 1, 4, and 5, as this would be in the direction of O'ahu's urbanized areas to the Southeast. Sample 1 recorded 185.84 MP m^{-2} d^{-1} with a wind direction of 132.16 degrees. Sample 4 also recorded Southeast winds (124.27°) and 180.55 particles m^{-2} d^{-1}. Precipitation was relatively low during both Samples 1 and 4 (< 0.6 mm d^{-1}). Sample 5 produced a relatively high deposition rate of 140.26 particles m^{-2} d^{-1} and had wind speeds of 13.01 mph originating from the Southeast (107.61°). Sample 5's precipitation was slightly elevated from Sample 4 by 1.75 mm d^{-1}. Like deposition rates in LM, Samples 6 and 7 recorded the lowest MP deposition rates; 65.18 and 73.50 MP m^{-2} d^{-1}, respectively, and the highest cumulative precipitation (0.943- and 3.19-mm d^{-1}). 3.2

3.4 SELECT SAMPLE PERIOD GRAPHS

Weather conditions during the first sampling period, displayed in Figure 14, show that both sites experienced the lowest precipitation during the entire experiment: 0.144 and 0.0642 mm d^{-1} in MAK and LM, respectively. Also, MAK and LM recorded the highest MP deposition rates of the experiment: 159 and 357 particles m^{-2} d^{-1} for MAK and LM, respectively. Winds in MAK recorded a high of about 18.1 mph and were primarily from the southeast. Because of the low precipitation rates and unhindered wind conditions during the first sample period, urban areas upwind are implicated as a potential source of MPs to MAK. LM experienced wind primarily from the NE, but about half of the frequency of winds originated from the SE at lower speeds of 14 to 18 mph.

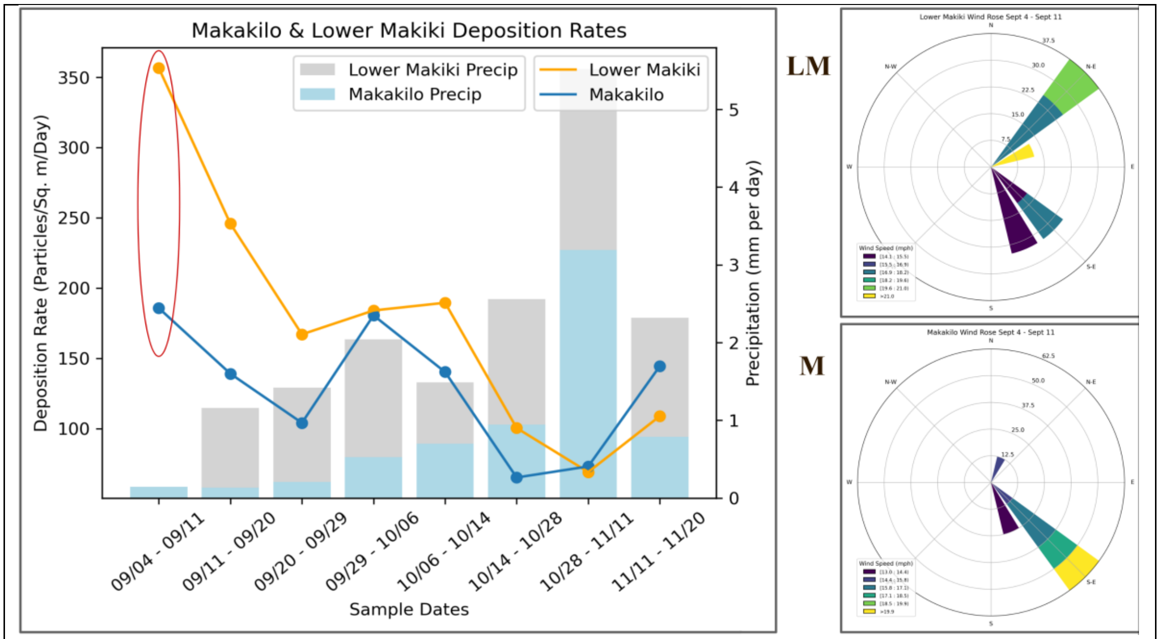

Figure 14. ***Overview of Weather Conditions: Sept 04 – Sept 11***

The graph on the left displays the microplastic deposition and precipitation rates for the entire experiment. The Windrose graphs display the wind conditions during the selected sampling period of September 04 – September 09. Windrose plots on the right display the wind conditions at both sampling sites. Windrose graphs were chosen to assist in analyzing MP sample counts compared to wind direction and identifying potential sources of atmospheric MPs. These graphs display the direction, frequency, and speed of the fastest 2-minute wind. The direction the wind originates is indicated by the direction of each spoke. The spokes' length represents the frequency of winds originating from any direction, and the colored segments within each spoke separate wind into a range of speeds that are described in the legend. See Appendix for a larger display of Windrose plots.

During sampling between September 29 – October 6, as seen in Figure 15, deposition rates at both sites are very similar, 180.6 and 184.1 particles m^{-2} d^{-1} for MAK and LM, respectively. The similarity in deposition rates could be a factor of the following: LMs experienced higher precipitation rates, 2.04 mm d^{-1}, roughly 1.5 mm d^{-1} more than MAK, recorded wind direction for LM primarily from the Northeast (>90°) with higher speed winds coming from the E at >23 mph, and winds in MAK originating exclusively from the Southeast.

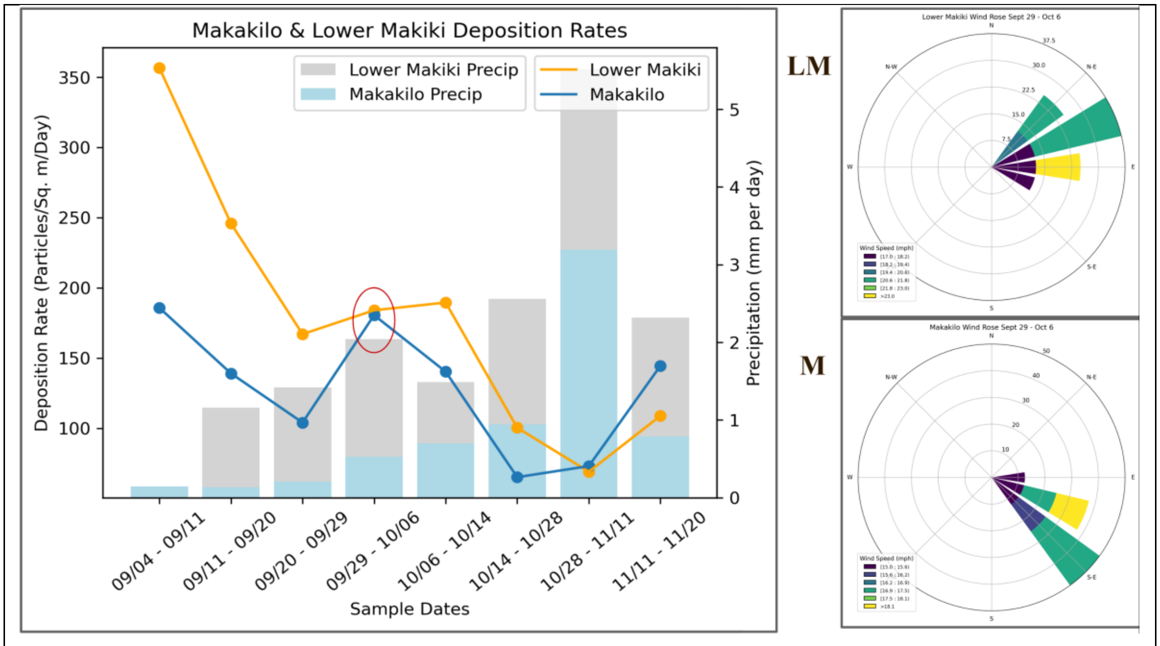

Figure 15. ***Overview of Weather Conditions: September 29 – October 06***

The graph on the left displays the microplastic deposition and precipitation rates for the entire experiment. The Windrose graphs display the wind conditions during the selected sampling period of September 29 – October 06. See the caption for Figure 14 for more information.

During the sampling period between October 28 – November 11, shown in Figure 16, MAKs deposition rates exceed LMs for the first time during this experiment. Once again, LM experienced higher precipitation rates (5.52 mm d^{-1}) than MAK (3.19 mm d^{-1}). Winds in LM were primarily from the Northeast with a smaller frequency of higher speed winds (>28 mph) coming from the east. During the same period, MAK received the majority of winds from the Northeast and East. However, the highest wind speeds during this period (>17 mph) were from the East and Southeast. Once again, this originates from the direction of higher population density areas.

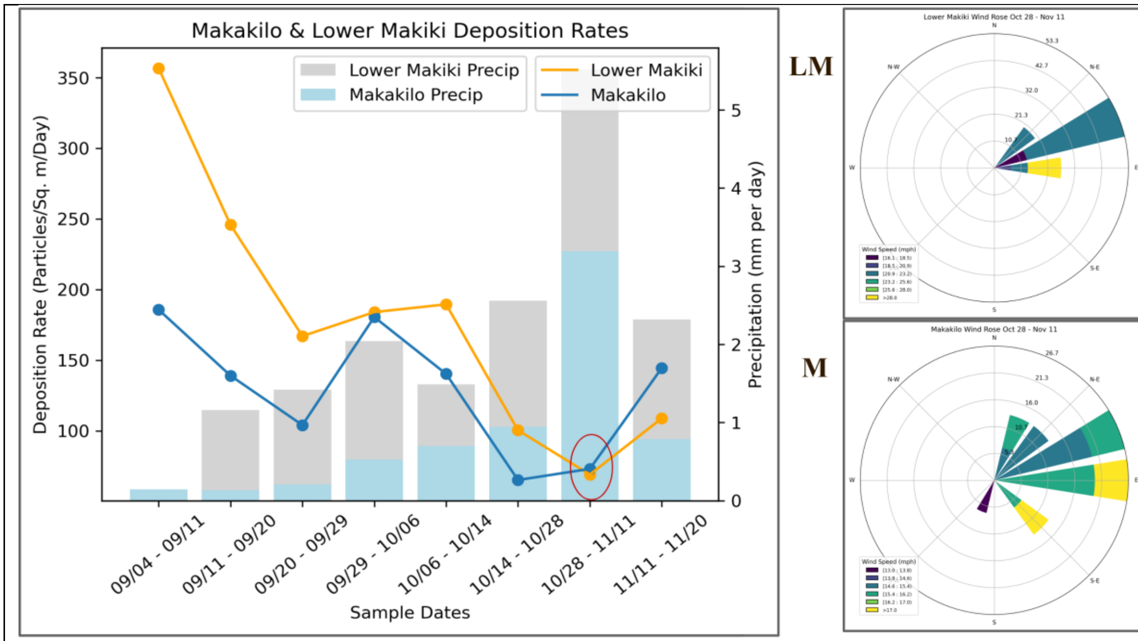

Figure 16. ***Overview of Weather Conditions: Oct 28 – Nov 11***

The graph on the left displays the microplastic deposition and precipitation rates for the entire experiment. The Windrose graphs display the wind conditions during the selected sampling period of October 28 – November 11. See the caption for Figure 14 for more information.

Shown in Figure 17, MAK continues to exceed LMs MP deposition rates between November 11 - November 20. Precipitation in LM, again, exceeds MAK by 1.54 mm d^{-1}, potentially reducing MP deposition. LMs wind direction is primarily from the Northeast, originating from the direction of typical trades. Winds in MAK are primarily from the East, signaling that high population density areas could have contributed MPs.

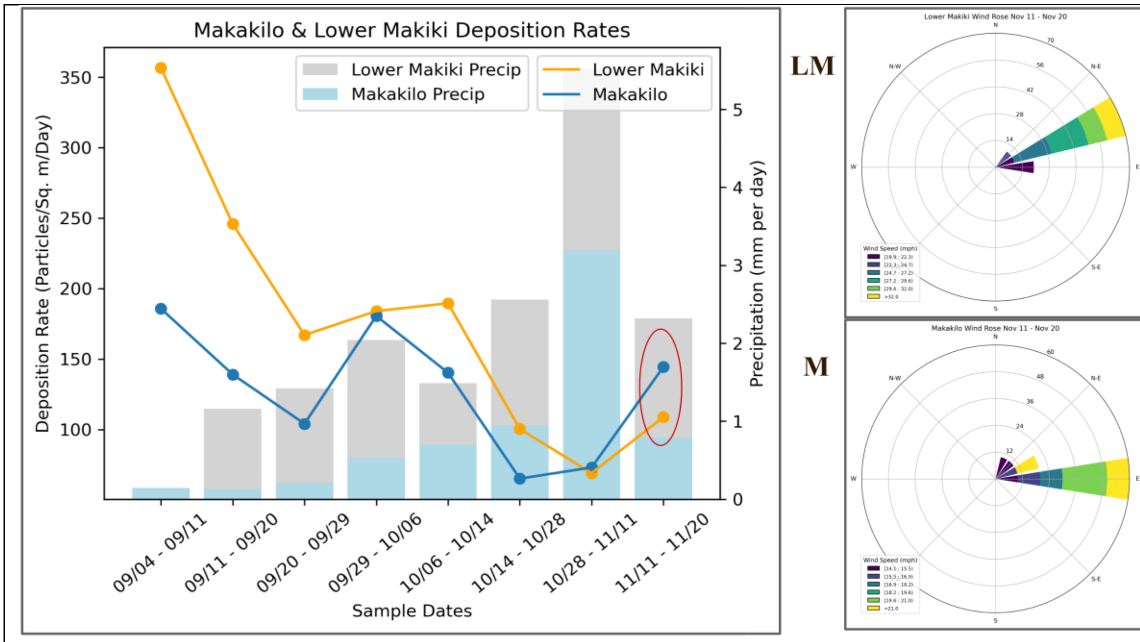

Figure 17. ***Overview of Weather Conditions: Nov 11 – Nov 20***

The graph on the left displays the microplastic deposition and precipitation rates for the entire experiment. The Windrose graphs display the wind conditions during the selected sampling period of October 28 – November 11. See the caption for Figure 14 for more information.

3.6 DATA ANALYSIS & VISUAL AIDS

3.6.1 PEARSON CORRELATIONS

Table 5. ***Pearson Correlations (n = 8)***

The Pearson correlation was calculated for each sample between the microplastic count and the variable given (wind speed, wind direction, or precipitation).

Selected Variables	Correlation Coefficient (r)	Magnitude of Correlation	P-value (p)	Significant (Y/N)
Honolulu counts (Observer 1 and 2):	0.960	Very strong	0.00223	Y
Makakilo counts (Observer 1 and 2):	0.681	Moderate	0.103	N
Correlation with Averaged MP Deposition Rates and Variables (MP m^{-2} d^{-1})				
Lower Makiki counts vs. wind speed	-0.676	Moderate	0.0656	N

Lower Makiki counts vs. wind direction	0.511	Moderate	0.196	N
Lower Makiki counts vs. precipitation	-0.752	Strong	0.031	Y
Makakilo counts vs. wind speed	0.612	Moderate	0.107	N
Makakilo counts vs. wind direction	0.470	Moderate	0.240	N
Makakilo counts vs. precipitation	-0.641	Moderate	0.087	N

The Pearson correlation analysis determines the strength of correlation between MP counts from Observer 1 and Observer 2, as well as the counts from both observers in comparison to wind direction and speed for each respective collection period. MP counts for observers 1 and 2 display significant correlations ($p < 0.05$). Unfortunately, MP counts at the MAK site did not meet the criteria for significance, though they had a correlation and p-value that were moderate in strength ($r = 0.681$, $p = 0.103$).

Pearson correlation analysis obtained by inputting the MP deposition rates averaged from observations 1 and 2 produced significant results when analyzing LM deposition rates and precipitation ($r = - 0.752$, $p = 0.031$). Moreover, Pearson correlation between LM's averaged deposition rates and wind speed produced nearly significant results ($r = -0.676$, $p = 0.066$), and though not as close to significance, wind direction correlation displayed moderate results ($r = 0.511$, $p = 0.196$). Larger sample sizes, increased sampling frequency, and removing outliers during larger precipitation events could improve Pearson correlation results further toward significance.

Correlation values from MAK, while not significant, also provided results suggesting a connection between MP deposition rates and environmental variables.

Precipitation had the lowest p-value (0.087) and an r-value of -0.641. The correlation between MP deposition rates, wind speed, and direction was r = 0.612, r = 0.470, respectively, with p-values of 0.107 and 0.240. Again, a larger sample size and increased frequency of sample collection may improve significance.

3.6.2 MP DEPOSITION RATES VS SELECT WEATHER VARIABLES

An easier way to view the connection between MP deposition rates and environmental variables is with scatter plots. Figure 18 displays MP deposition rates vs wind speed trend lines for LM and MAK. Surprisingly, the trendlines track in opposing directions. LM experiences a higher deposition rate with decreasing wind speeds, while MAK experiences a higher deposition rate with increasing wind speeds. Notably, LM experiences higher wind speeds than MAK, facilitating a significant distinction between data points in either location.

As shown in the middle graph in Figure 18, wind direction has a positive relationship with MP deposition rates. Both LM and MAK share this relationship. However, LM's MP deposition increases at a much faster rate, indicated by visual observation of the slopes of the respective trend lines. The wind directions all lie between 60 and 135 degrees – all easterly in direction – and wind directions from the southeast have higher deposition rates than wind directions from the northeast.

The deposition rate vs. precipitation graph in Figure 18 illustrates a negative relationship with MP deposition rates for both sampling sites. Additionally, LM experienced lower rates of precipitation and the greatest R^2 value of the two sites (R^2 =

0.68). When it rains during the sampling period, lower MP deposition rates are found as compared to dry sampling periods, which have higher MP deposition rates.

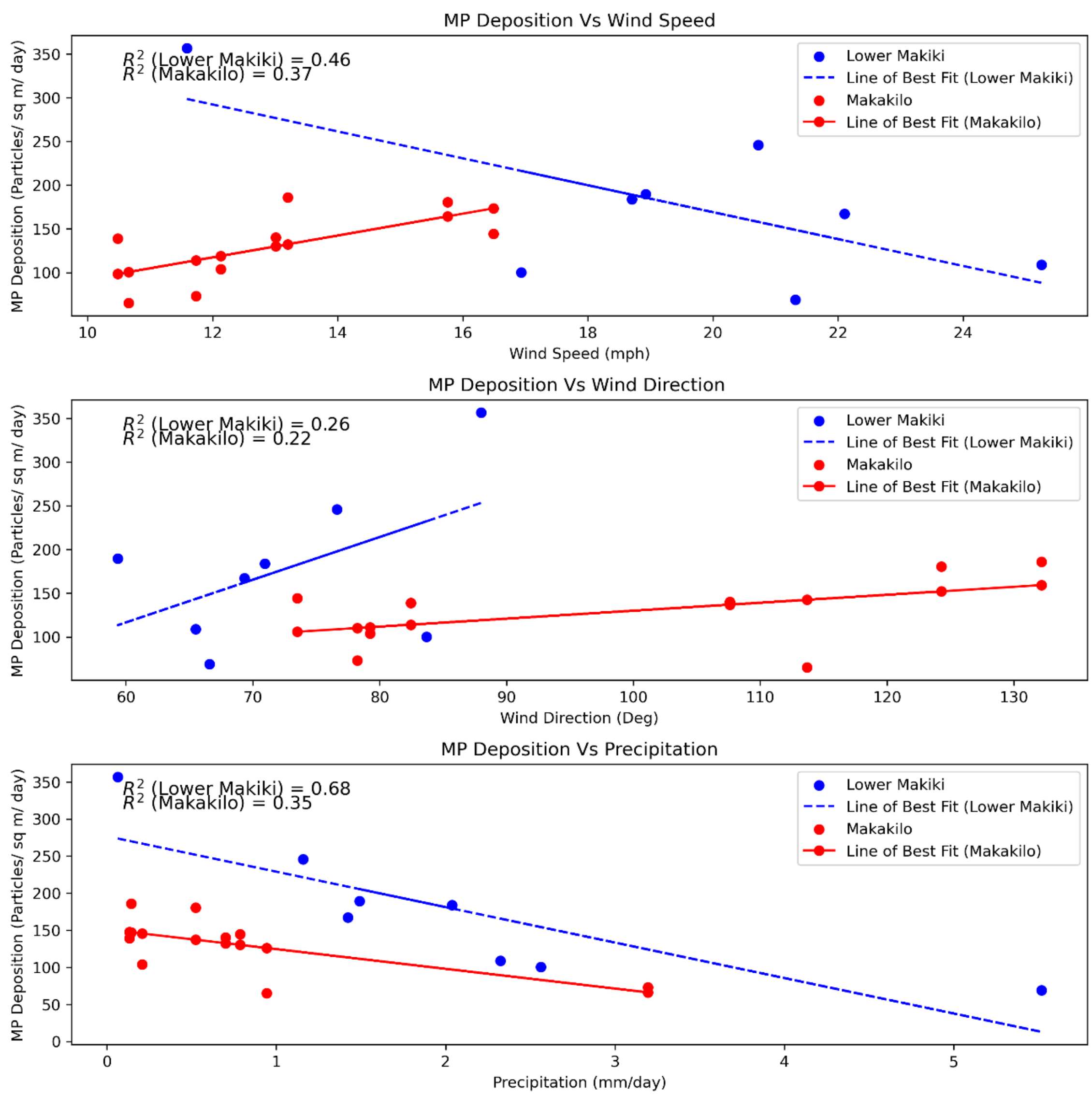

Figure 18. ***MP Deposition Rate vs Weather Variables in Lower Makiki and Makakilo*** Each graph displays the relationship between Lower Makiki and Makakilo MP deposition rates and selected weather variables, as well as the line of best fit and R^2 values for each location.

4.0 DISCUSSION

4.1 CORRELATION BETWEEN OBSERVER MP SAMPLE COUNTS

The MP counts between observers 1 and 2 is similar but could be improved upon. The LM location Pearson correlation analysis produced significant results ($r = 0.96$, $p = 0.00223$) while the MAK samples had lower Pearson Correlation values ($r = 0.681$, $r = 0.103$) between the two observer counts. With additional recounts, these Pearson Correlation values would hopefully increase. The MP counts are the backbone of this study, and recounts, or additional counters, would provide additional confidence in the results of this study.

4.2 CHALLENGES AND UNCERTAINTIES IN MP IDENTIFICATION

In addition to MP counting, other challenges in this study include the considerable time investment required to prep materials (samplers, filters, MP extraction, microscope observation, etc.). Each phase involved several hours more than anticipated, dedicated to each task. This was especially the case for microscope observations. Each sample required between 1 - 4 hours each depending on the number of MPs and other debris on each sample. Furthermore, MP identification using a microscope can be highly subjective without proper preparation and familiarization with the physical characteristics of MPs. We learned this the hard way with a third untrained observer whose counts were not included in this analysis. Furthermore, many objects can be misidentified as MPs, increasing the potential for error and increasing the variability of MP counts between observers. In the case of this study, recounts were necessary to improve MP count accuracy and correlation between counts from both observers. While counts were kept independent, occasional meetings between the counters to discuss commonly seen particles were helpful. As such, future research using similar methods to quantify MPs in the environment should be done with a small team, with a minimum of 2 people from beginning to end. Additionally, team members should increase along with the scale of the study. This would ensure a timely execution of all required tasks and potentially increase the frequency of sample collection throughout a study. Moreover, efforts must be made to train observers about the many forms, colors, shapes, and other characteristics of MPs to reduce possible errors in counting and increase the confidence of future studies.

4.3 REMOTE AREAS OBSERVE LOWER MP DEPOSITION RATES

Following previous studies on deposition rates in remote and suburban areas, MAK also experienced lower MP deposition rates compared to the higher density area of LM. This could be the result of several factors: greater use of plastic products coinciding with larger populations, larger concentrations of cars in the area, larger concentrations of synthetic clothing, etc. With the potential that this is the case, MAK may be spared higher MP deposition rates should its urban density remain relatively low. However, urban Honolulu may act as a source of MPs. Therefore, limiting population density in MAK may not be the only way to reduce MP fallout.

The highest deposition rates for both locations occurred when winds originated in the direction of higher density areas to the East and South-East. This indicates that high population density areas in this direction may contribute MPs to remote areas, depending upon wind trajectories. More sampling would need to be done to confirm this hypothesis, however, literature suggests that this is no coincidence. In lieu of sufficient samples, an investigation into the role of wind speed would provide further evidence to support the urban-sourced-MP theory.

4.4 WINDS DRIVE MP DEPOSITION IN LOWER MAKIKI & MAKAKILO

In the case of LM, greater wind speeds produce lower deposition rates, and vice versa for MAK. Setting aside periods of significant rainfall, this relationship suggests that higher wind speeds are necessary to suspend and transport MPs sourced from urban areas to the East or Southeast of the MAK sampling site. Additionally, higher wind speeds may facilitate the suspension and dispersal of larger micro-scale plastic particles originating from densely populated areas, potentially allowing a greater range of particle sizes to be deposited in remote areas. Therefore, because MAK is situated as such, higher wind speeds originating from urban areas may be necessary to generate sufficient force to offset or delay MP settling velocity and disperse MPs from more densely populated areas to the elevated sampling site in MAK.

During sampling periods in LM where wind speeds reduce from the prior sampling period, MP deposition rates increase. Because LM has densely populated areas directly East, greater amounts of MPs can accumulate in the atmosphere and be deposited once winds begin to subside. This pattern corroborates the conclusions of Wright et al. (2020), Liu et al. (2019), Allen et al. (2019), and Yang et al. (2025), displaying the potential for lower wind speeds to allow suspended particles to settle in urban areas and limit the dispersal range of larger micro-scale plastics.

Though more studies are needed to confirm the speculative findings of this experiment, the data trends and patterns suggest that the MP suspension and deposition pathways on Oʻahu are likely to follow the pathways as described by Can-Güven (2020). However, expanded sample sizes and observation methods that identify the size distribution of MPs are needed to determine the weather conditions necessary to suspend particles of varying sizes and densities. Additionally, because the wind direction rarely diverges from the direction of the trade winds, it is also difficult to rule out other potential sources (other populated areas to the Northeast, and potentially the Great Pacific Garbage Patch).

4.5 PRECIPITATION LIMITS MP DEPOSITION

Precipitation data provide further evidence to support the exogenous nature of MPs in MAK. Considering the concept of in-cloud and sub-cloud scavenging, it appears that these processes contribute negligible amounts of MPs to both locations. During sample periods with the highest cumulative precipitation, the lowest deposition rates are recorded. This could indicate that the troposphere's MP reservoir over either site is not sufficient in affecting deposition rates during precipitation events. Moreover, the relationship between precipitation and deposition rates indicates that rainfall may prevent new atmospheric MPs from entering precipitation zones rather than contributing to the deposition rate through in-cloud or sub-cloud scavenging. Conversely, it is also likely that precipitation may limit the suspension of particles in densely populated areas, reducing the contribution of MPs to the atmospheric reservoir. In any case, research is needed to further contextualize the pacifying effect of precipitation on MP deposition rates and the significance of unhindered wind-driven MP suspension.

4.6 INVESTIGATION OF STORM EVENTS ON MP DEPOSITION

While wind speed alone may likely affect MP deposition rates of either location, there also appears to be an interesting anomaly in the data trend that suggests that higher wind speeds during precipitation events may also contribute to increasing deposition rates during sample periods. This can be observed during Samples 7 and 8 in LM and MAK. During these sample periods, increasing wind speeds and moderately high precipitation rates were observed. This observation inspires further investigation into the relationship between precipitation and wind speed on MP dispersal pathways. Though extremely speculative, a combination of elevated wind speeds and sub-cloud scavenging may accelerate the deposition, suspension, or resuspension pathways as described above, and increase the dispersal range of MPs in comparison to typical precipitation events.

Tropical storms and their predicted increase in frequency due to climate change provide opportunities to observe changes in MP deposition rates and dispersal pathways in severe weather conditions. Continued sampling during storm events and evaluating wind and precipitation, along with MP deposition rates, could provide additional insight into the extent of the mitigating effect of precipitation on atmospheric MP suspension and dispersal pathways on Oʻahu.

4.7 SUGGESTIONS FOR REMEDIATION EFFORTS

Additional findings from this study suggest that areas that are consistently downwind from urbanized areas are likely to experience higher MP fallout rates. This could threaten native agricultural practices, water quality, and agricultural productivity because of the ability of MPs to alter soil microbial communities and nutrient content. Therefore, this study finds that areas downwind of urbanized areas should be investigated to determine the effects of plastic pollution on soil health, if any, and to determine appropriate measures to reduce prolonged damage. However, it may prove futile to combat any effects or initiate remediating measures considering the projected increase in plastic production in the future and the increasingly ubiquitous nature of MPs in the environment as they degrade from their primary source. Nevertheless, Hawaiʻi's most densely populated areas provide a starting point for any initiative to reduce plastic pollution across the island.

4.8 SUGGESTIONS FOR FUTURE RESEARCH

Further investigation is needed to corroborate the findings of this study. Most notably, increasing the time frame of the study and sampling frequency alongside site-specific weather observations would greatly increase the validity of experiments of this nature. Moreover, expanding sampling to more areas around the island, including ocean-based experiments, can aid in providing additional context in determining the direction and location of MP sources. If possible, samples gathered from Oʻahu's Northeast coast could provide insight regarding the contribution of MPs from the ocean. This may be of importance considering Hawaiʻi's proximity to the Great Pacific Garbage Patch (GPGP) and dominance of trade winds in the state. Additionally, further investigation into the effects of storm events on the dispersal and deposition of MPs could be increasingly relevant as the frequency of storms increases due to climate change factors.

5.0 CONCLUSION

This study finds that areas with greater population densities observe greater amounts of atmospheric MP deposition than more remote and sparsely populated areas. This is likely due to the higher concentration of plastic products, tire wear, washing, and weathering of synthetic clothing, litter, etc. The MPs derived from these sources can be suspended at greater rates with increasing wind speed. Increased wind speeds also facilitate the spread of MPs across the island, threatening remote areas and ecosystems downwind. However, the effectiveness of wind-facilitated MP dispersal may be hindered by the onset of precipitation events, which, in theory, remove suspended MP particles and limit travel distance. Though these findings are limited by their low sample count, if true, they would indicate that areas with greater population densities are the top priority targets for MP pollution reduction efforts. Further research is needed to expand the base of knowledge of the intricacies of MP dispersal pathways and potential methods to mitigate the seemingly inevitable spread of MPs across the island.

APPENDIX

WINDROSE GRAPHS

Figure 19. ***Windrose Graphs – Kalaeloa Airport***

Windrose Graphs were chosen to assist in analyzing MP sample counts in comparison to wind direction, assisting in identifying potential sources of atmospheric MPs. These graphs display the direction, frequency, and speed of the fastest 2-minute wind. The direction the wind originates is indicated by the direction of each spoke. The spokes' length represents the frequency of winds originating from any particular direction, and the colored segments within each spoke separate wind into a range of speeds that are described in the legend.

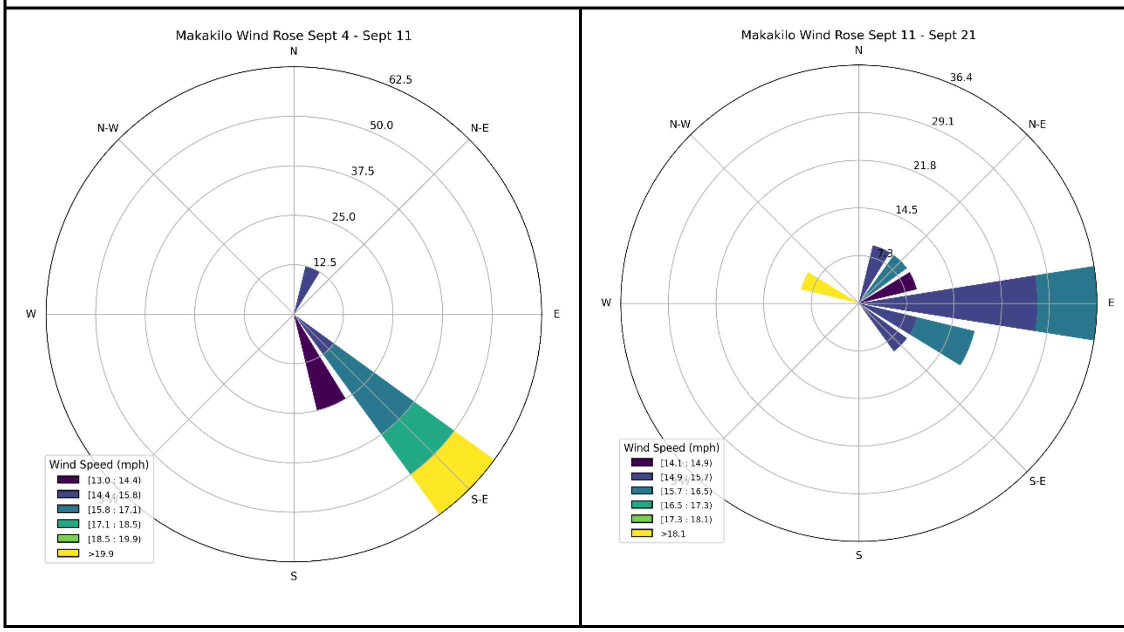

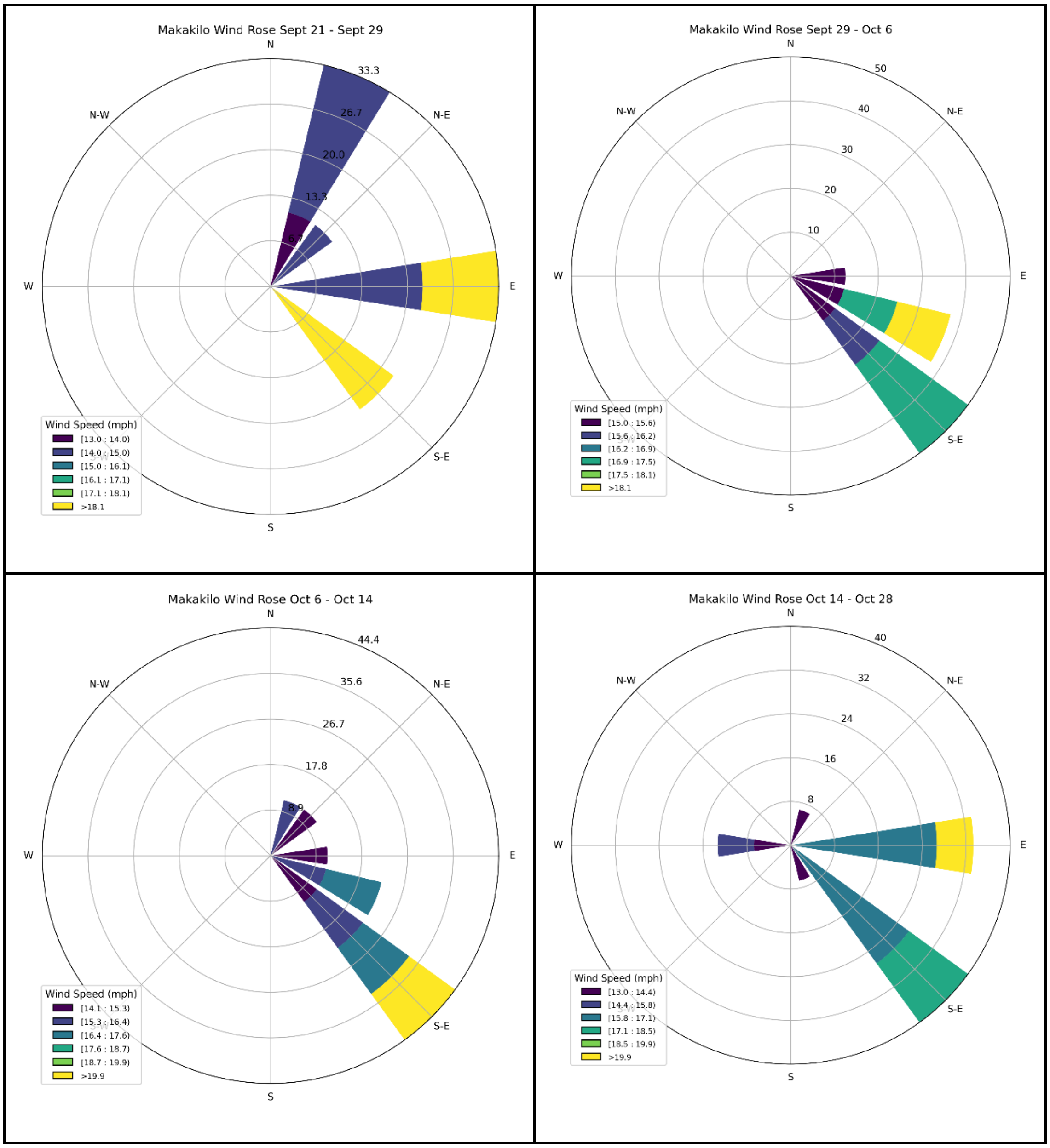
Makakilo Wind Rose Sept 21 - Sept 29
N
N-E
E
S-E
S
W
N-W
33.3
26.7
20.0
13.3
6.7
Wind Speed (mph)
[13.0 : 14.0)
[14.0 : 15.0)
[15.0 : 16.1)
[16.1 : 17.1)
[17.1 : 18.1)
>18.1
Makakilo Wind Rose Sept 29 - Oct 6
N
N-E
E
S-E
S
W
N-W
50
40
30
20
10
Wind Speed (mph)
[15.0 : 15.6)
[15.6 : 16.2)
[16.2 : 16.9)
[16.9 : 17.5)
[17.5 : 18.1)
>18.1
Makakilo Wind Rose Oct 6 - Oct 14
N
N-E
E
S-E
S
W
N-W
44.4
35.6
26.7
17.8
8.9
Wind Speed (mph)
[14.1 : 15.3)
[15.3 : 16.4)
[16.4 : 17.6)
[17.6 : 18.7)
[18.7 : 19.9)
>19.9
Makakilo Wind Rose Oct 14 - Oct 28
N
N-E
E
S-E
S
W
N-W
40
32
24
16
8
Wind Speed (mph)
[13.0 : 14.4)
[14.4 : 15.8)
[15.8 : 17.1)
[17.1 : 18.5)
[18.5 : 19.9)
>19.9

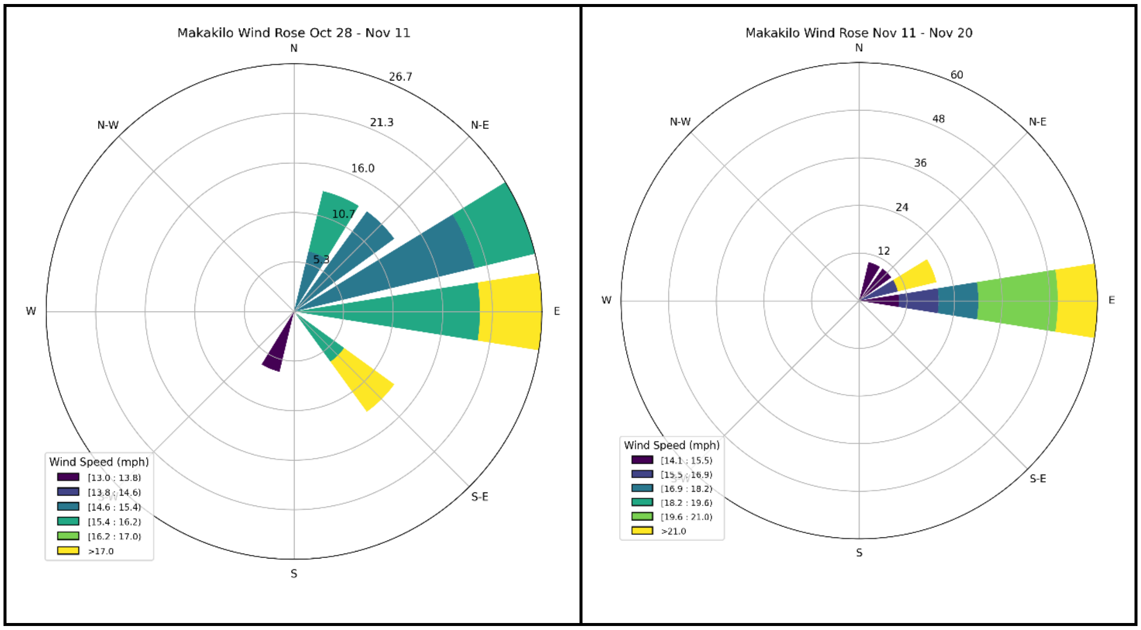

Figure 20. ***Windrose Graphs - Honolulu Int. Airport***

Windrose Graphs were chosen to assist in analyzing MP sample counts in comparison to wind direction, assisting in identifying potential sources of atmospheric MPs. These graphs display the direction, frequency, and speed of the fastest 2-minute wind. The direction the wind originates is indicated by the direction of each spoke. The spokes' length represents the frequency of winds originating from any particular direction, and the colored segments within each spoke separate wind into a range of speeds that are described in the legend.

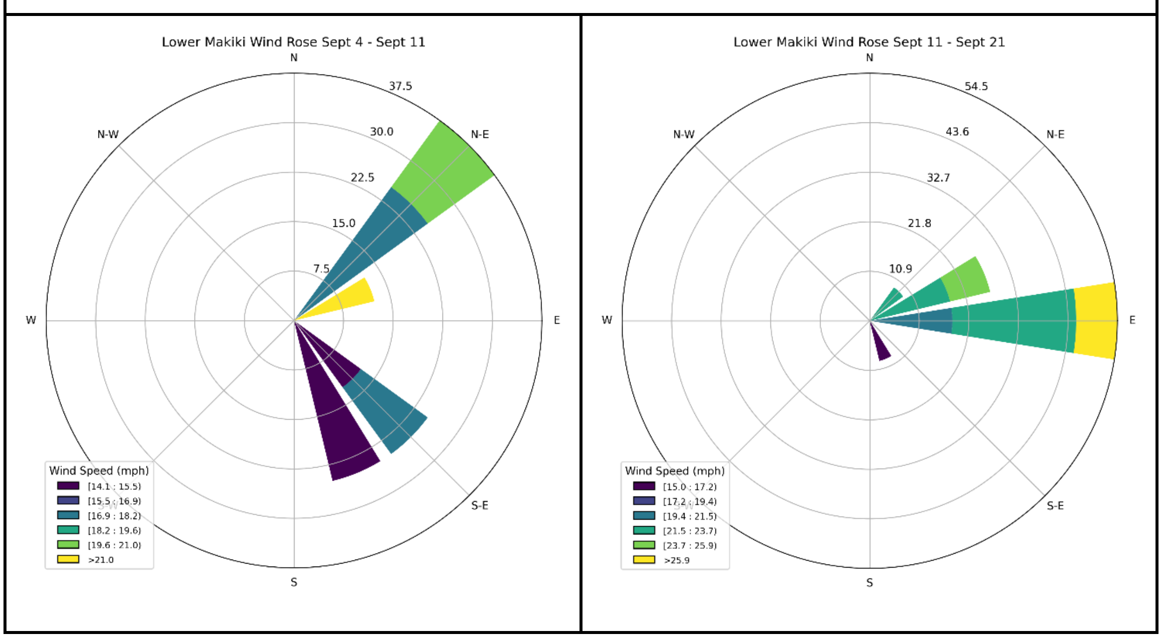

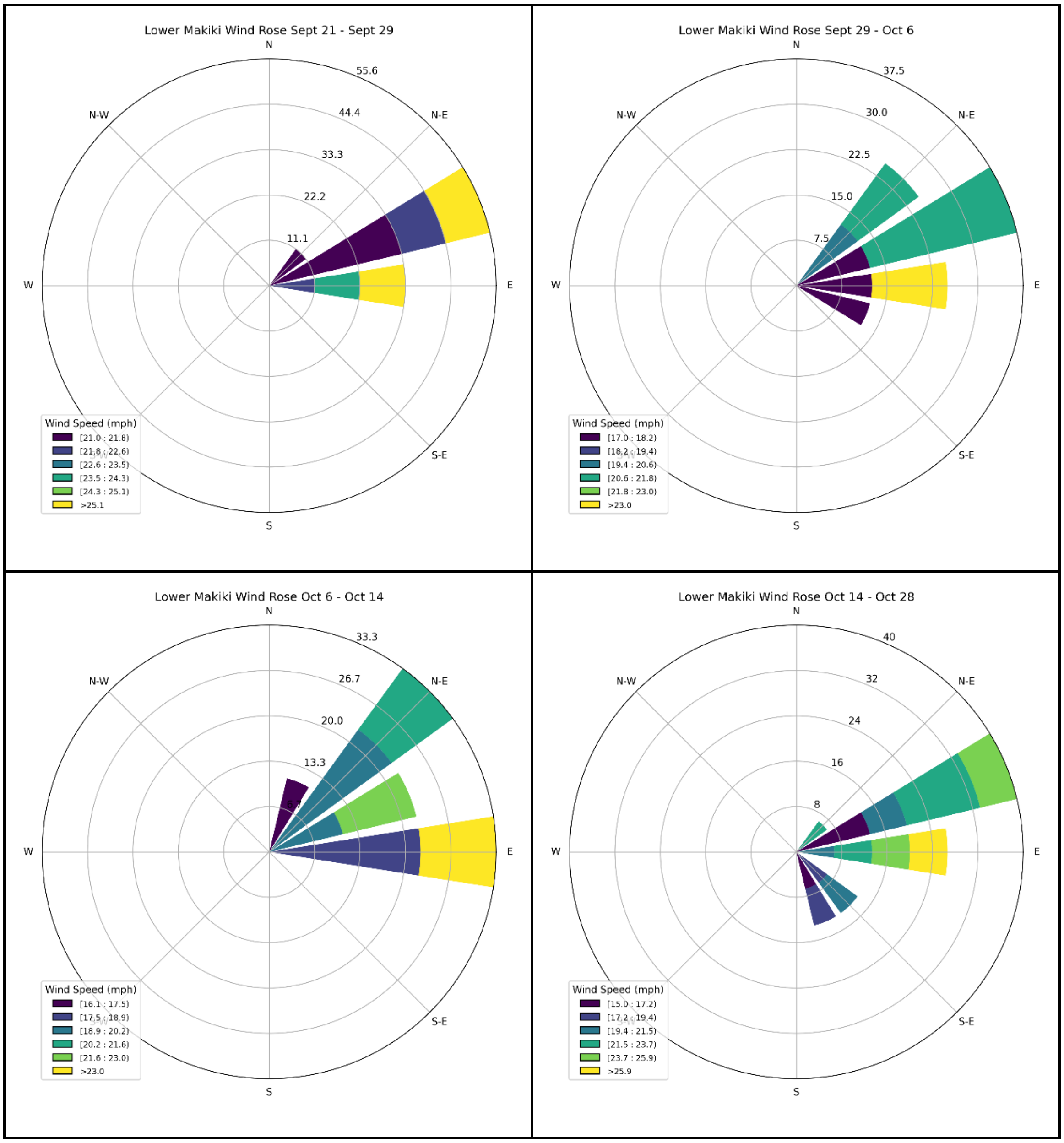
Lower Makiki Wind Rose Sept 21 - Sept 29
N
N-E
E
S-E
S
W
N-W
11.1
22.2
33.3
44.4
55.6
Wind Speed (mph)
[21.0 : 21.8)
[21.8 : 22.6)
[22.6 : 23.5)
[23.5 : 24.3)
[24.3 : 25.1)
>25.1
Lower Makiki Wind Rose Sept 29 - Oct 6
N
N-E
E
S-E
S
W
N-W
7.5
15.0
22.5
30.0
37.5
Wind Speed (mph)
[17.0 : 18.2)
[18.2 : 19.4)
[19.4 : 20.6)
[20.6 : 21.8)
[21.8 : 23.0)
>23.0
Lower Makiki Wind Rose Oct 6 - Oct 14
N
N-E
E
S-E
S
W
N-W
13.3
20.0
26.7
33.3
Wind Speed (mph)
[16.1 : 17.5)
[17.5 : 18.9)
[18.9 : 20.2)
[20.2 : 21.6)
[21.6 : 23.0)
>23.0
Lower Makiki Wind Rose Oct 14 - Oct 28
N
N-E
E
S-E
S
W
N-W
8
16
24
32
40
Wind Speed (mph)
[15.0 : 17.2)
[17.2 : 19.4)
[19.4 : 21.5)
[21.5 : 23.7)
[23.7 : 25.9)
>25.9

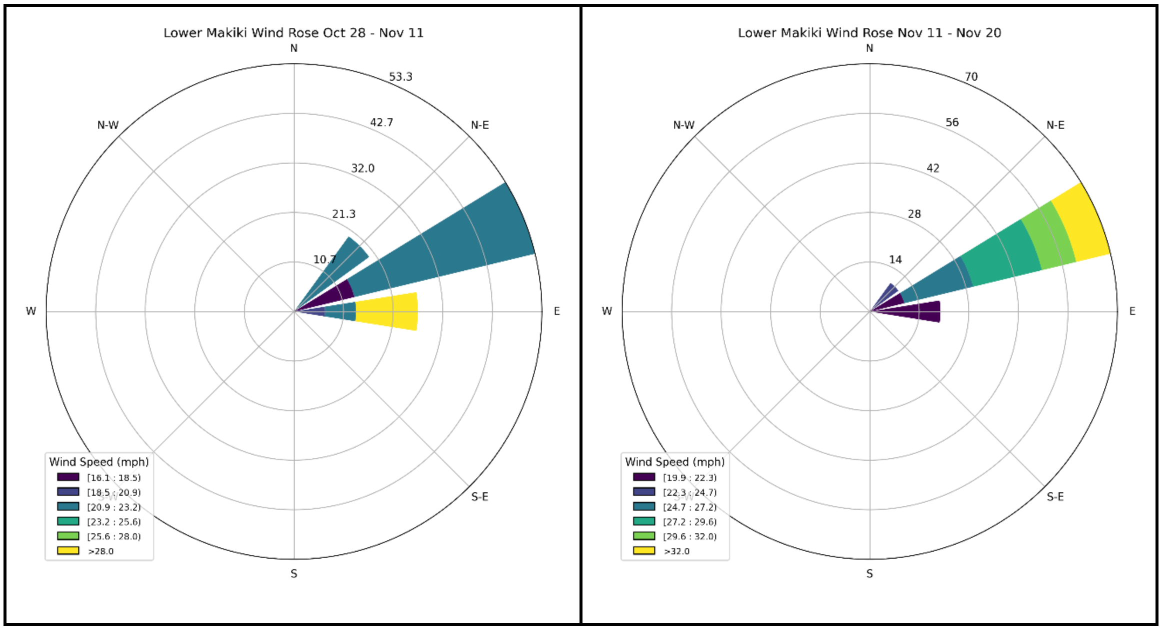
Lower Makiki Wind Rose Oct 28 - Nov 11
N
N-E
E
S-E
S
W
N-W
10.7
21.3
32.0
42.7
53.3
Wind Speed (mph)
[16.1 : 18.5)
[18.5 : 20.9)
[20.9 : 23.2)
[23.2 : 25.6)
[25.6 : 28.0)
>28.0
Lower Makiki Wind Rose Nov 11 - Nov 20
N
N-E
E
S-E
S
W
N-W
14
28
42
56
70
Wind Speed (mph)
[19.9 : 22.3)
[22.3 : 24.7)
[24.7 : 27.2)
[27.2 : 29.6)
[29.6 : 32.0)
>32.0

LITERATURE CITED

Aeschlimann, Mischa, et al. “Potential Impacts of Atmospheric Microplastics and Nanoplastics on Cloud Formation Processes.” *Nature Geoscience*, vol. 15, no. 12, Nov. 2022, pp. 967–75, https://doi.org/10.1038/s41561-022-01051-9.

Allen, Steve, et al. “Atmospheric Transport and Deposition of Microplastics in a Remote Mountain Catchment.” *Nature Geoscience*, vol. 12, no. 5, Apr. 2019, pp. 339–44, https://doi.org/10.1038/s41561-019-0335-5.

Allen Steve et al. “Examination of the Ocean as a Source for Atmospheric Microplastics.” *PLOS ONE*, edited by Amitava Mukherjee, vol. 15, no. 5, May 2020, p. e0232746, https://doi.org/10.1371/journal.pone.0232746. Accessed 12 July 2020.

Aralappanavar, Vijay Kumar, et al. “Effects of Microplastics on Soil Microorganisms and Microbial Functions in Nutrients and Carbon Cycling – a Review.” *Science of the Total Environment*, vol. 924, Elsevier BV, May 2024, pp. 171435–35, https://doi.org/10.1016/j.scitotenv.2024.171435.

Can-Güven, Emine. “Microplastics as Emerging Atmospheric Pollutants: A Review and Bibliometric Analysis.” *Air Quality, Atmosphere & Health*, vol. 14, Sept. 2020, pp. 203–15, https://doi.org/10.1007/s11869-020-00926-3.

“Census Reporter.” *Census Reporter*, 2023, censusreporter.org/profiles/86000US96822-96822/. Accessed 17 Mar. 2025.

Chen, Guanglong, et al. “An Overview of Analytical Methods for Detecting Microplastics in the Atmosphere.” *TrAC Trends in Analytical Chemistry*, vol.

130, Sept. 2020, p. 115981, https://doi.org/10.1016/j.trac.2020.115981. Accessed 30 Nov. 2020.

"Data Portal – Hawaiʻi Climate Data Portal." *www.hawaii.edu*, www.hawaii.edu/climate-data-portal/data-portal/.

Dris, Rachid, et al. "Synthetic Fibers in Atmospheric Fallout: A Source of Microplastics in the Environment?" *Marine Pollution Bulletin*, vol.. 104, no. 1-2, Mar. 2016, pp. 290–93, https://doi.org/10.1016/j.marpolbul.2016.01.006.

Gambino, Isabella, et al. "Occurrence of Microplastics in Tap and Bottled Water: Current Knowledge." *International Journal of Environmental Research and Public Health*, vol. 19, no. 9, Apr. 2022, p. 5283, https://doi.org/10.3390/ijerph19095283.

Geyer et al. (2017); OECD (2022) – with major processing by Our World in Data. "Annual plastic production between 1950 and 2019" [dataset]. Geyer et al., "Production, use, and fate of all plastics ever made"; OECD, "Global Plastics Outlook - Plastics use by application" [original data].

Ghaffar, Imania, et al. "Plastics in the Environment as Potential Threat to Life: An Overview." *Environmental Science and Pollution Research*, vol. 29, no. 38, June 2022, pp. 56928–47, https://doi.org/10.1007/s11356-022-21542-x.

"Global Plastic Production with Projections." *Our World in Data*, ourworldindata.org/grapher/global-plastic-production-projections.

Guide to Microplastics Identification: A Comprehensive Methods Guide for Microplastics Identification and Quantification in the Laboratory 30 YEARS of ENVIRONMENTAL IMPACT RESEARCH. 2019, www.shawinstitute.org/sites/default/files/uploaded/Shaw%20Institute%202019%2C%20Guide%20to%20Microplastic%20Identification.pdf.

Khuyen, Vo, et al. “Assessing Microplastic Prevalence and Dispersion from Saigon Urban Canals via Can Gio Mangrove Reserve to East Sea by Raman Scattering Microscopy.” *Microplastics*, vol. 1, no. 3, Sept. 2022, pp. 536–53, https://doi.org/10.3390/microplastics1030038. Accessed 15 Oct. 2024.

Klein, Malin, and Elke K. Fischer. “Microplastic Abundance in Atmospheric Deposition within the Metropolitan Area of Hamburg, Germany.” *Science of the Total Environment*, vol. 685, Oct. 2019, pp. 96–103, https://doi.org/10.1016/j.scitotenv.2019.05.405. Accessed 4 Sept. 2020.

NOAA. “National Centers for Environmental Information (NCEI).” *Noaa.gov*, 2019, www.ncei.noaa.gov/. Accessed 24 Dec. 2024.

Ryan, Anna C., et al. “Transport and Deposition of Ocean-Sourced Microplastic Particles by a North Atlantic Hurricane.” *Communications Earth & Environment*, vol. 4, no. 1, Nov. 2023, pp. 1–10, https://doi.org/10.1038/s43247-023-01115-7.

Vijay Kumar Aralappanavar, et al. “Effects of Microplastics on Soil Microorganisms and Microbial Functions in Nutrients and Carbon Cycling – a Review.” *Science of the Total Environment*, vol. 924, Elsevier BV, May 2024, pp. 171435–35, https://doi.org/10.1016/j.scitotenv.2024.171435.

Zhang, Kai, et al. “Understanding Plastic Degradation and Microplastic Formation in the Environment: A Review.” *Environmental Pollution*, vol. 274, Apr. 2021, p. 116554, https://doi.org/10.1016/j.envpol.2021.116